NASA Technical Paper 1744

Stability Boundaries for Systems With Frequency-Model Feedback and Complementary Filter

L. Keith Barker

NASA

Stability Boundaries for Systems With Frequency-Model Feedback and Complementary Filter

L. Keith Barker
Langley Research Center
Hampton, Virginia

SUMMARY

General parameter-plane equations are derived to generate stability bound-
aries for a class of systems characterized by a feedback loop that contains a
complementary filter and a model for either the low- or high-frequency portion
of the plant. This combination allows those frequencies of the part of the
plant that is modeled to be fed back for control while suppressing other
frequencies.

For all specific examples considered, the stability regions obtained using
the complementary filter and frequency model were larger (and in some cases,
considerably larger) than those obtained using a low-pass filter in the feed-
back of the system output. Furthermore, higher gain control was possible.

INTRODUCTION

A filter can be thought of as a circuit, a differential equation, or a
transfer function which passes certain frequencies in an input while attenuat-
ing or rejecting others. The specific filter discussed in this paper is
referred to as a complementary filter. It consists of two subfilters - a
high-pass filter and a corresponding low-pass filter - the outputs of which
are summed.

A primary application of the complementary filter is as follows. Suppose
two different sensors are used to measure a state of a system. Moreover, let
the first instrument be good at measuring the high-frequency content of the
signal but not the low-frequency content. In other words, the first instrument
records the signal plus a low-frequency noise. The second instrument gives an
accurate indication of the signal at the low frequencies but degrades at the
higher frequencies (high-frequency noise). One approach is to pass the signal
from the first instrument through a high-pass filter and the signal from the
second instrument through a low-pass filter and then sum the results to get a
representation of the whole signal. The only constraint placed on this system
by the complementary filter is that the transfer functions of the high-pass and
the low-pass filters must sum to unity. Under ideal conditions of no noise,
a signal which passes through a complementary filter will be reproduced exactly.
No distortion or phase shift will occur in the signal. However, with noise,
this will not be the case. With a noisy input, parameters in the complementary
filter are adjusted so that the total impurity from the low-frequency noise in
the first instrument and the high-frequency noise in the second instrument is
minimized.

The complementary filter is a simple concept, but at the same time, it is
a very powerful and useful concept. The complementary filter in earlier work
(refs. 1 and 2) is referred to as a "distortionless" filter. According to the
editorial comment in reference 1, this type of filter enjoyed much success in
a variety of applications around 1956. It has applications in aircraft flight

measurements and inertial navigation (refs. 3, 4, and 5). A compensation-filtering scheme was used in reference 3 to significantly increase the band-width of an early Skylab control-moment-gyro system configuration by combining noisy position-sensor information and "clean" rate-command information. For practical reasons, the rate command was used instead of the actual system rate. In this sense, the compensation filter is a complementary filter. Brown (ref. 4) discussed the relationship of the complementary filter to the Kalman filter. Higgins (ref. 6) continued this comparison and showed that the complementary filter is a special case of a steady-state Kalman filter. Schmidt (ref. 7) compared the complementary and Kalman filters for the STOLAND system. It is important to note at this point that application of the complementary filter does not require any knowledge of the more complex Kalman filter.

Accurate mathematical models of the high-frequency modes of a system are not always available. Consequently, in a control design based on models of the low-frequency modes, it may be undesirable to feed back the very high frequencies, which were not taken into account in the control design. Also, in flexible booster control, it is important not to set up any resonance with the structural mode of the system. At the same time, however, it is desired to control the rigid-body modes. A novel and ingenious use of the complementary filter was made by Tutt and Waymeyer (ref. 8) in flexible booster control: "This approach does not adapt to body bending, but instead is contrived to ignore it . . ." by using the basic concept of the complementary filter and a rigid-body model in the feedback loop. This same basic idea was recently applied in the high-vibration environment of a helicopter to eliminate low-frequency rotor-induced vibrations (refs. 9 and 10). This latter work used a high-frequency plant model.

The objective of this paper is to apply the parameter-plane method (ref. 11) to derive stability boundary equations for a particular class of systems (defined by a general block diagram), which use the Tutt and Waymeyer (ref. 8) feedback approach. The parameter-plane method is used to display the stability region in the two-dimensional space of a parameter of the complementary filter and a control gain. Specific examples are presented, and a standard low-pass filter feedback is used for comparison.

SYMBOLS

$A(I,J)$ matrix element in the Ith row and Jth column

A function of S defined in deriving explicit expressions for K
               and T

A_R, A_I real and imaginary parts of A, respectively

B function of S defined in deriving explicit expressions for K
               and T

B_R, B_I real and imaginary parts of B, respectively

C	function of S defined in deriving explicit expressions for K and T
C_R, C_I	real and imaginary parts of C, respectively
D	function of S defined in deriving explicit expressions for K and T
D_R, D_I	real and imaginary parts of D, respectively
$D(I)$	denominator of the Ith transfer function $G(I)$
$\tilde{D}(S)$	denominator of system transfer function $H(S)$
$D(S)$	characteristic equation, or denominator of $H(S)$ relatively prime to $N(S)$
$F(S)$	Laplace transform of input signal to complementary filter
$G(I)$	transfer function of the Ith system
$H(S)$	system transfer function
h	high-frequency noise
i	$= \sqrt{-1}$
I,J	integers
K	system control gain constant
K_1, K_2	particular values of K
ℓ	low-frequency noise
M	function defined in equation (37)
$N(I)$	numerator of the Ith transfer function $G(I)$
$\tilde{N}(S)$	numerator of system transfer function $H(S)$
$N(S)$	numerator of $H(S)$ relatively prime to $D(S)$
S	Laplace complex variable
$|S|$	absolute value of S
T	parameter in low-pass and high-pass filters
T_1, T_2	particular values of T

t	time
$U(S)$	Laplace transform of system input
X_L, X_H	outputs of low-frequency and high-frequency plant models, respectively
$(X_H)_{LP}$	X_H after passing through low-pass filter
$X(S)$	Laplace transform of system output
$Y(S)$	Laplace transform of output signal from complementary filter
α, β, γ	functions defined in equations (33), (34), and (35), respectively
λ, μ	quantities which take on the values of either unity or negative unity
σ	real part of S
ω	imaginary part of S

ANALYSIS

The complementary filter is briefly discussed, then the system block diagram for the present analysis is presented, followed by a formulation of the characteristic equation of the system. Using this characteristic equation for the block diagram, the parameter-plane method (ref. 11) is used to develop general equations for generating stability boundaries in the plane defined by a filter parameter and the system control gain. Stable regions are identified from these stability boundaries.

Complementary Filter

Figure 1 shows the complementary filter operating on an uncorrupted signal $F(S)$ and having an output $Y(S)$. Since $H(S)$ and $1 - H(S)$ occur in parallel, the resultant transfer function is given by their sum, which is unity - hence, the name complementary filter. The point to be made from figure 1 is this: If a signal $F(S)$ passes through a high-pass filter with transfer function $H(S)$ and a low-pass filter with transfer function $1 - H(S)$, which are complementary, and if the signals from the two filters are summed, then the output signal $Y(S)$ will be the same as the input signal $F(S)$. There is no distortion or phase shift of the input.

Figure 2 shows a complementary filter with noisy inputs. Suppose ℓ is a low-frequency noise and h is a high-frequency noise. The output is described by

$$Y(S) = H(S)\left[F(S) + \ell\right] + \left[1 - H(S)\right]\left[F(S) + h\right]$$

$$= F(S) + \left\{H(S)\ell + \left[1 - H(S)\right]h\right\} \tag{1}$$

4

Notice in equation (1) that $Y(S) = F(S)$ except for the residual error term in the braces.

Figure 3 shows the specific form of the complementary filter of interest in this paper. Equation (1) becomes

$$Y(S) = F(S) + \left(\frac{TS}{TS + 1}\right)\ell + \left(\frac{1}{TS + 1}\right)h \tag{2}$$

In signal processing, the problem is to choose T to minimize the residual error. The following section uses the same filter components shown in figure 3 but with different inputs to accomplish a desired objective. The influence of T on system stability is emphasized.

Frequency Feedback Model With Complementary Filter

Figure 4 shows the system block diagram examined in this paper. The system has an input $U(S)$ and an output $X(S)$. The overall plant is composed of low-frequency and high-frequency plants preceded by a servo. The complementary filter consists of the specific high-pass and low-pass filters shown in figure 3. The objective is to examine stability regions in the plane of the filter parameter T and the system gain K.

The operation depicted in figure 4 is explained as follows: Let X_L and X_H be the outputs of the low-frequency plant and high-frequency plant, respectively. If the low-frequency plant model and servo model are exact models, then the output of the low-frequency plant model will also be X_L. Notice that the input to the high-pass filter component of the complementary filter is X_L, while $X_L + X_H$ is the input to the low-pass filter component. Since X_L passes through both the high-pass filter and low-pass filter components of the complementary filter, it will be unchanged. Meanwhile, X_H passes through the low-pass filter. Hence, as shown, the resultant feedback is $X_L + (X_H)_{LP}$, that is, the output of the low-frequency plant plus the output from the high-frequency plant which has been passed through a low-pass filter. The term $(X_H)_{LP}$ is the low-frequency part of the high-frequency plant. Adjusting T adjusts the low-frequency part of X_H that is fed back for control. This paper examines the effect of K and T on system stability.

Characteristic Equation

The notation in figure 4 is convenient for deriving general expressions involving the system transfer functions. The $N(I)$'s and $D(I)$'s are the numerators and denominators, respectively, of the block transfer functions.

The system transfer function between $X(S)$ and $U(S)$ in figure 4 is denoted by

$$\frac{X(S)}{U(S)} = H(S) \qquad (3)$$

with

$$H(S) = \frac{\tilde{N}(S)}{\tilde{D}(S)} = \frac{N(S)}{D(S)} \qquad (4)$$

where $\tilde{N}(S)$ and $\tilde{D}(S)$ signify polynomials in S which may have some common factors that can be canceled. The numerator N(S) of the transfer function and the denominator D(S) have no common factors and are mathematically said to be relatively prime polynomials in S.

The polynomial D(S) is referred to as the characteristic polynomial, and D(S) = 0 is called the characteristic equation. Roots of D(S) are called characteristic roots. It is well known that a linear, time-invariant system is stable (X(t) → 0 as t → ∞) if and only if all roots of the characteristic equation have negative real parts.

The system transfer function H(S), expressed in terms of the individual G(I) block transfer functions in figure 4, is easily shown to be

$$H(S) = \frac{K[G(1) + G(2)]G(6)}{1 + K[G(4)\ G(5)\ G(7) + G(1)\ G(3)\ G(6) + G(2)\ G(3)\ G(6)]} \qquad (5)$$

Replacing the G(I)'s in equation (5) with their equivalent ratios shown in figure 4 allows equation (5) to be written as equation (4) with

$$\tilde{N}(S) = K[N(1)\ D(2) + D(1)\ N(2)]N(6)\ D(1)\ D(2)\ D(3)\ D(4)\ D(5)\ D(6)\ D(7) \qquad (6)$$

$$\tilde{D}(S) = D(1)\ D(2)\ D(6)\{D(1)\ D(2)\ D(3)\ D(4)\ D(5)\ D(6)\ D(7)$$

$$+ K[D(1)\ D(2)\ D(3)\ N(4)\ N(5)\ D(6)\ N(7)$$

$$+ N(1)\ D(2)\ N(3)\ D(4)\ D(5)\ N(6)\ D(7)$$

$$+ D(1)\ N(2)\ N(3)\ D(4)\ D(5)\ N(6)\ D(7)]\} \qquad (7)$$

Notice in figure 4 that

6

$$N(4) = TS \tag{8}$$

$$D(4) = D(3) \tag{9}$$

$$N(3) = 1 \tag{10}$$

$$D(3) = TS + 1 \tag{11}$$

For perfect modeling, $G(5) = G(1)$, and $G(7) = G(6)$; therefore,

$$N(5) = N(1) \tag{12}$$

$$D(5) = D(1) \tag{13}$$

$$N(7) = N(6) \tag{14}$$

$$D(7) = D(6) \tag{15}$$

For convenience, equation (6) is expressed as

$$\tilde{N}(S) = D(1)\ D(2)\ D(4)\ D(5)\ D(6)\ D(7)\ N(S) \tag{16}$$

where

$$N(S) = K[N(1)\ D(2) + D(1)\ N(2)]D(3)\ N(6) \tag{17}$$

Equations (9), (13), and (15) allow equation (7) to be factored as

$$\tilde{D}(S) = D(1)\ D(2)\ D(4)\ D(5)\ D(6)\ D(7)\ D(S) \tag{18}$$

where

$$D(S) = D(1)\ D(2)\ D(3)\ D(6) + K[D(2)\ N(4)\ N(5)\ N(7)$$
$$+ N(1)\ D(2)\ N(3)\ N(6) + D(1)\ N(2)\ N(3)\ N(6)] \tag{19}$$

The ratio of N(S) to D(S) is the system transfer function. Recall that D(S) = 0 is the characteristic equation. By equations (8), (10), (11), (12), and (14), the characteristic equation can be expressed as

$$D(1) \ D(2) \ (TS + 1) \ D(6) + K[D(2) \ (TS) \ N(1) \ N(6) + N(1) \ D(2) \ N(6)$$
$$+ \ D(1) \ N(2) \ N(6)] = 0 \tag{20}$$

A more convenient and compact form of the characteristic equation for application of the parameter-plane method is

$$TA + KTB + KD + C = 0 \tag{21}$$

where

$$A = S[(D(1) \ D(2) \ D(6)] \tag{22}$$

$$B = S[D(2) \ N(1) \ N(6)] \tag{23}$$

$$C = D(1) \ D(2) \ D(6) \tag{24}$$

$$D = N(1) \ D(2) \ N(6) + D(1) \ N(2) \ N(6) \tag{25}$$

The values of S which satisfy equation (20) or equation (21) are the characteristic roots. Clearly, these roots will vary as K and T take on different values. The parameter-plane method is used to examine how the stability condition (stable or unstable) changes with different combinations of K and T.

Stability Boundaries

In this section, equations are derived to generate stability boundaries in the plane of K and T for the system shown in figure 4. For comparative purposes, similar equations are developed for a low-pass filter feedback system. This latter system is the same as the system in figure 4, except that the path through the servo model, frequency model, and high-pass filter is removed.

Complementary filter system.- The numerators and denominators of the block transfer functions in figure 4 are functions of S. Consequently, A, B, C, and D in equations (22) to (25) are functions of S. Let S = iω and write A, B, C, and D as complex numbers:

$$A = A_R + iA_I \tag{26}$$

$$B = B_R + iB_I \tag{27}$$

$$C = C_R + iC_I \tag{28}$$

$$D = D_R + iD_I \tag{29}$$

Substituting equations (26) to (29) into equation (21) and setting the resulting real and imaginary parts equal to zero yields the two simultaneous equations for K and T:

$$TA_R + K(TB_R + D_R) + C_R = 0 \tag{30}$$

$$TA_I + K(TB_I + D_I) + C_I = 0 \tag{31}$$

Subtract equation (31) multiplied by $(TB_R + D_R)$ from equation (30) multiplied by $(TB_I + D_I)$ to get the quadratic equation in T:

$$\alpha T^2 + \beta T + \gamma = 0 \tag{32}$$

where

$$\alpha = B_I A_R - B_R A_I \tag{33}$$

$$\beta = D_I A_R + B_I C_R - D_R A_I - B_R C_I \tag{34}$$

$$\gamma = D_I C_R - D_R C_I \tag{35}$$

The roots of equation (32) are

$$T = \frac{-\beta \pm \sqrt{M}}{2\alpha} \tag{36}$$

where

$$M = \beta^2 - 4\alpha\gamma \tag{37}$$

The two roots in equation (36) are denoted as T_1 for the positive radical and as T_2 for the negative radical. The gain K, obtained by adding equations (30) and (31), is

$$K = - \frac{T(A_R + A_I) + C_R + C_I}{T(B_R + B_I) + D_R + D_I} \tag{38}$$

In equation (38), $K = K_1$ when $T = T_1$, and $K = K_2$ when $T = T_2$.

At this point, it may be worthwhile to state explicitly the meaning of equations (36) and (38). For particular constant values of K and T, the characteristic equation will have a set of corresponding roots. As K and T are varied, these roots will move, generating root-locus curves. Suppose it is desired to find values for K and T which result in a root-locus curve intersecting the imaginary axis at some specified point $S = i\omega^*$, where ω^* is a particular value of ω. This is accomplished by setting $S = i\omega^*$ in the characteristic equation, equating the real and imaginary parts to zero, and solving the two resulting simultaneous equations for K and T.

Equations (36) and (38) produce those combination values of K and T which will result in a root-locus curve intersecting the imaginary axis at $S = i\omega$. For a given value of ω, the value of T is calculated from equation (36), which is an implicit function of ω. Then, K is calculated from equation (38) using this value of T and the same value of ω. By letting ω vary, a plot of K versus T can be generated. The resulting curves are stability boundaries that correspond to the imaginary axis in the S-plane. Hence, in the same manner that the imaginary axis divides the S-plane into a stable region (left half-plane) and an unstable region (right half-plane), the stability boundaries partition the plane of K and T into stable and unstable regions.

Since only real values of T are of practical interest, calculations are only continued for $M \geq 0$ in equation (37). Also, since the characteristic roots occur in complex-conjugate pairs, it is sufficient to plot T versus K as ω increases from zero. Using negative values of ω would only duplicate the results obtained for positive values of ω.

Low-pass filter system.- The low-pass filter system is the same as the system shown in figure 4, except that the path passing through the servo model, frequency model, and high-pass filter is omitted. It can be shown that the associated characteristic equation is

$$D(S) = D(1)\ D(2)\ D(3)\ D(6) + K[N(1)\ D(2)\ N(3)\ N(6)$$

$$+ D(1)\ N(2)\ N(3)\ N(6)] = 0 \tag{39}$$

10

Equations (10) and (11) permit equation (39) to be written as

$$D(1)\ D(2)\ (TS + 1)\ D(6) + K\big[N(1)\ D(2)\ N(6) + D(1)\ N(2)\ N(6)\big] = 0 \qquad (40)$$

or, in the more convenient form,

$$A(TS + 1) + KB = 0 \qquad (41)$$

where

$$A = D(1)\ D(2)\ D(6) \qquad (42)$$

$$B = \big[N(1)\ D(2) + N(2)\ D(1)\big] N(6) \qquad (43)$$

Setting $S = i\omega$ and using the complex representations for A and B (eqs. (26) and (27)) modifies equation (41) to

$$(A_R + iA_I)Ti\omega + (A_R + iA_I) + K(B_R + iB_I) = 0 \qquad (44)$$

Setting the real and imaginary parts in equation (44) equal to zero results in the two simultaneous equations:

$$-A_I T\omega + A_R + KB_R = 0 \qquad (45)$$

$$A_R T\omega + A_I + KB_I = 0 \qquad (46)$$

The simultaneous solutions of equations (45) and (46) are

$$T = \frac{A_R B_I - B_R A_I}{\omega(A_I B_I + B_R A_R)} \qquad (47)$$

$$K = \frac{-\left(A_R{}^2 + A_I{}^2\right)}{A_R B_R + A_I B_I} \qquad (48)$$

In equations (47) and (48), T and K are single-valued functions of ω.

Zero characteristic roots.- It is only natural that in solving for T to obtain equations (36) and (47), division by zero is encountered. This follows because T always appears with S in the transfer functions for the low-pass and high-pass filters in figure 4. With S = iω, one can think about solving for ωT and then dividing by ω to get an equation for T. The ω is shown explicitly in the denominator of equation (47) for emphasis. Hence, in generating the stability boundaries, special attention must be given to the question: What combination values of T and K result in the characteristic equation having zero roots (S = 0)? The computer program which formed the system characteristic equation from the component transfer functions and then solved for its roots used the following convenient notation.

Let

$$N(1) = A(1,1) + A(1,2)S + A(1,3)S^2 + \ldots \tag{49}$$

$$D(1) = A(2,1) + A(2,2)S + A(2,3)S^2 + \ldots \tag{50}$$

and so forth. Then, form the matrix where the first row contains the coefficients of the polynomial N(1), the second row the coefficients of the polynomial D(1), etc. Symbolically,

$$
\begin{array}{l}
N(1) \\
D(1) \\
N(2) \\
D(2) \\
N(3) \\
D(3) \\
N(4) \\
D(4) \\
N(5) \\
D(5) \\
N(6) \\
D(6) \\
N(7) \\
D(7)
\end{array}
\begin{bmatrix}
A(1,1) & A(1,2) & A(1,3) & \cdots \\
A(2,1) & A(2,2) & A(2,3) & \cdots \\
A(3,1) & \cdots & & \\
A(4,1) & \cdots & & \\
A(5,1) & \cdots & & \\
A(6,1) & \cdots & & \\
A(7,1) & \cdots & & \\
A(8,1) & \cdots & & \\
A(9,1) & \cdots & & \\
A(10,1) & \cdots & & \\
A(11,1) & \cdots & & \\
A(12,1) & \cdots & & \\
A(13,1) & \cdots & & \\
A(14,1) & \cdots & &
\end{bmatrix}
\tag{51}
$$

The constant term for N(l) is A(l,l); for D(l), is A(2,l), etc. Using
this notation and setting S = 0 in equation (20) gives

$$K = \frac{-A(2,1)\ A(4,1)\ A(12,1)}{A(1,1)\ A(4,1)\ A(11,1) + A(2,1)\ A(3,1)\ A(11,1)} \tag{52}$$

For later applications, N(6) = 1 or A(11,1) = 1, so that equation (52)
reduces to

$$K = \frac{-A(2,1)\ A(4,1)\ A(12,1)}{A(1,1)\ A(4,1) + A(2,1)\ A(3,1)} \tag{53}$$

When K has the value computed using equation (53), the characteristic
equation has a root on the imaginary axis at the origin, regardless of the value
of T. This constant value of K, for arbitrary value of T, is plotted also
in the parameter plane as a stability boundary. In the K,T plot, this special
boundary appears as a vertical line which intersects the K-axis at the value
assigned by equation (53).

Infinite characteristic roots.- To obtain the stability boundaries associ-
ated with infinite characteristic roots, the combination values of T and K
which satisfy the characteristic equation when $|S| = |i\omega| \to \infty$ are computed.
This is accomplished by dividing the characteristic equation by its maximum
power in S. Afterwards, the only term not having some power of S in the
denominator is the original coefficient of the maximum power of S. Hence, as
$|S| \to \infty$, this coefficient approaches zero in order to satisfy the remaining
characteristic equation.

For all subsequent applications, the maximum power of S in the charac-
teristic equation will occur in the D(1) D(2) (TS) D(6) term in equations (20)
and (40). After dividing by the maximum power of S and afterwards letting
$|S| \to \infty$, there remains a constant term times T equated to zero. After divid-
ing by this constant term, T = 0. The result is that T = 0 and K arbitrary
is a stability boundary, that is, the K-axis.

Stability Regions

As the coordinating parameter $\omega > 0$ increases in the set of equations
developed for K and T, a plot of T versus K can be drawn as, for example,
in figure 5. This partitions the T,K plane into different regions which are
either stable or unstable. The stability condition of a given region is then
evaluated by choosing a point inside the region and computing the characteris-
tic roots for this point. The number of roots with positive real parts
(unstable roots) in each region is circled in figure 5. A circled zero indi-

cates a stable region. The number of unstable roots gained or lost in moving from one region to another is evident. In subsequent applications, only the stable regions are emphasized.

Calculation Procedure

Figure 6 illustrates the general procedure used to construct the stability regions for the complementary-filter system. First, a set of transfer functions for the blocks in figure 4 is input to a computer program. Next, the quantities ω, M, T_1, K_1, T_2, and K_2 are obtained from a computer printout generated by incrementing ω. From this printout, values of ω for which $M \geq 0$ are selected for further consideration. The program has options for plotting T_1 versus K_1 or T_2 versus K_2. To generate the stability boundaries (T versus K curves), ω is incremented in the range where $M \geq 0$, and values of T (eq. (36)) are plotted against corresponding values of K (eq. (38)). These boundaries can be overlooked if this incrementation interval for ω is too large. Efficient generation of the stability boundaries requires close monitoring of the computer printout and plotter by the investigator.

The same procedure is followed for the low-pass filter system. The program has an option for selecting either the complementary or low-pass filter system. For the low-pass filter, equations (47) and (48) are pertinent.

Degree of Stability

In this paper, the substitution $S = i\omega$ is used to generate stability boundaries. For values of K and T falling within the stable regions, confined by these boundaries, there are no characteristic roots located on or to the right of the imaginary axis in the S-plane. In a similar manner, stability regions could be generated such that for combination values of K and T falling within these regions, there are no roots any closer to the imaginary axis than some specified number σ. This is accomplished by setting $S = \sigma + i\omega$ and following the same procedure described in this paper. For further reading on relative stability, refer to references 11 and 12.

High-Frequency Plant Model

A low-frequency plant model is indicated in figure 4 because the objective was ultimately, through use of the complementary filter, to filter out the high frequencies from the feedback signal.

In reference 9, it was desired to filter out the low frequencies; hence, a high-frequency plant model was used. To use the equations of this paper for a high-frequency plant model, simply call G(1) the high-frequency plant, G(2) the low-frequency plant, and G(5) the high-frequency plant model, and interchange G(3) and G(4).

Approximation Models

All numerical results presented in this paper are based on perfect models of the servo and low-frequency plant of the real system. To examine the effects of modeling errors, equations (12) to (15) should not be used. This translates into the fact that equation (21) still holds, except that

$$A = S[D(1)\ D(2)\ D(5)\ D(6)\ D(7)] \tag{54}$$

$$B = S[D(1)\ D(2)\ N(5)\ D(6)\ N(7)] \tag{55}$$

$$C = D(1)\ D(2)\ D(5)\ D(6)\ D(7) \tag{56}$$

$$D = N(1)\ D(2)\ D(5)\ N(6)\ D(7) + D(1)\ N(2)\ D(5)\ N(6)\ D(7) \tag{57}$$

Equations (54) to (57) allow variations in the models G(7) and G(5) from those of G(6) and G(1), respectively. Everything else remains the same. There are no changes in the equations corresponding to the low-pass filter system.

The flight investigation of reference 9, which used a high-frequency plant model, reported that the " . . . overall system performance was insensitive to mismatch between the dynamics of the plant and the plant model used in the complementary filter computation."

APPLICATIONS

The overall plant is composed of two subplants, a high-frequency plant and a low-frequency plant. Arbitrary plant transfer functions are assigned for numerical computation. For the high-frequency plant,

$$\frac{N(2)}{D(2)} = \frac{0.3S^2 + 0.45S + 0.9}{S^2 + 0.06S + 9} \tag{58}$$

and, for the low-frequency plant:

$$\frac{N(1)}{D(1)} = \frac{2S + 1}{S^2 + 1.4\lambda S + \mu} \tag{59}$$

where λ and μ are either 1 or - 1.

Four special cases are enumerated based on the denominator term in the low-frequency plant:

Case 1: $S^2 + 1.4S + 1$ (stable plant: $\lambda = 1$, $\mu = 1$)

Case 2: $S^2 - 1.4S + 1$ (unstable plant: $\lambda = -1$, $\mu = 1$)

Case 3: $S^2 + 1.4S - 1$ (unstable plant: $\lambda = 1$, $\mu = -1$)

Case 4: $S^2 - 1.4S - 1$ (unstable plant: $\lambda = -1$, $\mu = -1$)

Stability regions resulting from feedback implementing a low-pass filter are compared graphically with those from feedback incorporating the complementary filter in figure 4. Plots are presented for two conditions: (1) without servo (figs. 7 to 10) and (2) with servo (figs. 11 to 14).

Without Servo

Case 1.- Figure 7 shows the block diagram and stable regions resulting from use of the low-pass filter and the complementary filter. Comparing figures 7(b) and 7(c) shows the improvement brought about by using the complementary filter. Especially note that larger K values are permitted. In effect, larger K values mean tighter control because K enhances the system error so that it can be further reduced.

The stability boundaries in figure 7(b) and 7(c) intersect the K-axis at the same points. This will always be the case, because for T = 0 in figure 4, the complementary filter reduced to the low-pass filter.

Case 2.- The low-frequency plant has negative damping and is unstable. The block diagram and stability regions are shown in figures 8. Note the negligible stable region for the low-pass filter in figure 8(b) and the vast improvement in figure 8(c) for the complementary filter.

Case 3.- The results in figure 9 show a larger stable region for the complementary filter.

Case 4.- Figure 10 displays a tremendous improvement in the size of the stability boundary when the complementary filter is used over that when the low-pass filter is used.

With Servo

The block diagrams in figures 11, 12, 13, and 14 are the same as those in figures 7, 8, 9, and 10, respectively, except for the servo and servo model. The same basic conclusions persist, namely, (1) the system with the complementary filter has a larger stable region in the K,T plane than the system with only a low-pass filter and (2) for a given value of T, a stable system can be

maintained while using larger error gains K for tighter control. Incidentally, figure 11(b) corresponds to the stable region shown in figure 5 for $T \geq 0$.

CONCLUDING REMARKS

A complementary filter is commonly used in signal processing to estimate a state or signal when more than one measurement of the state is available. In previous work, the complementary filter has been used in conjunction with a model of the rigid-body modes for flexible booster control. This approach allows the structural modes to be filtered from the feedback signal, while the low-frequency rigid-body modes are not.

In this paper, general parameter-plane equations are derived to generate stability boundaries for a class of systems characterized by a feedback loop that contains a complementary filter and a model for either the low- or high-frequency portion of the plant. This combination allows those frequencies of the part of the plant that is modeled to be fed back for control while suppressing other frequencies. The plant and model rational transfer functions can be specified arbitrarily.

Numerical examples are presented which compare the stability regions obtained using the complementary-filter-model system with those regions incurred in using just a standard low-pass filter feedback. For the selected examples, it is shown that the complementary-filter-model system produces a larger stability region and allows larger error gains (tighter control or regulation) to be used.

Langley Research Center
National Aeronautics and Space Administration
Hampton, VA 23665
September 9, 1980

REFERENCES

1. Stewart, R. M.; and Parks, R. J.: Degenerate Solutions and an Algebraic Approach to the Multiple-Input Linear Filter Design Problem. IRE Trans. Circuit Theory, vol. CT-4, no. 1, Mar. 1957, pp. 10-14.

2. Bendat, Julius S.: Optimum Filters for Independent Measurements of Two Related Perturbed Messages. IRE Trans. Circuit Theory, vol. CT-4, no. 1, Mar. 1957, pp. 14-19.

3. Anderson, W. W.; Avis, L. M.; and Jacobs, K. L.: ATM-CMG Control System Stability. NASA TM-81827, 1980.

4. Brown, R. G.: Integrated Navigation Systems and Kalman Filtering - A Perspective. Presented at 28th Annual Meeting Inst. Navigation (West Point, N.Y.), June 27-29, 1972.

5. Stengel, Robert F.; Broussard, John R.; and Berry, Paul W.: The Design of Digital-Adaptive Controllers for VTOL Aircraft. NASA CR-144912, 1976.

6. Higgins, Walter T., Jr.: A Comparison of Complementary and Kalman Filtering. IEEE Trans. Aerosp. & Electron. Syst., vol. AES-11, no. 3, May 1975, pp. 321-325.

7. Schmidt, Stanley F.: A Kalman Filter for the STOLAND System. NASA CR-137668, 1975.

8. Tutt, G. E.; and Waymeyer, W. K.: Model Feedback Applied to Flexible Booster Control. IRE Trans. Automat. Contr., vol. AC-6, no. 2, May 1961, pp. 135-142.

9. Garren, John F., Jr.; Niessen, Frank R.; Abbott, Terence S.; and Yenni, Kenneth R.: Application of a Modified Complementary Filtering Technique for Increased Aircraft Control System Frequency Bandwidth in High Vibration Environment. NASA TM X-74004, 1977.

10. Niessen, F. R.; and Garren, J. F., Jr.: Filtering Technique Based on High-Frequency Plant Modeling for High-Gain Control. U.S. Patent 4,148,452, Apr. 1979.

11. Popov, E. P.: The Dynamics of Automatic Control Systems. Addison-Wesley Pub. Co., Inc., 1962.

12. Siljak, Dragoslav D.: Nonlinear Systems. John Wiley & Sons, Inc., c.1969.
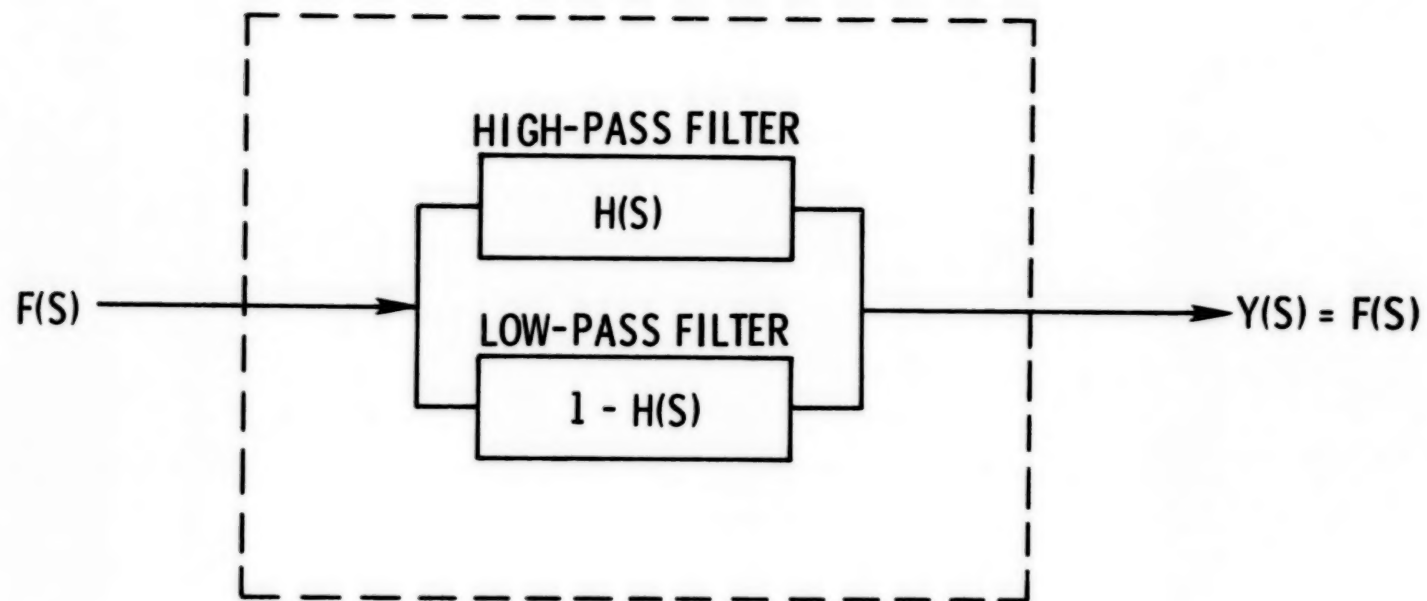
Figure 1.- Complementary filter with noise-free input signal.
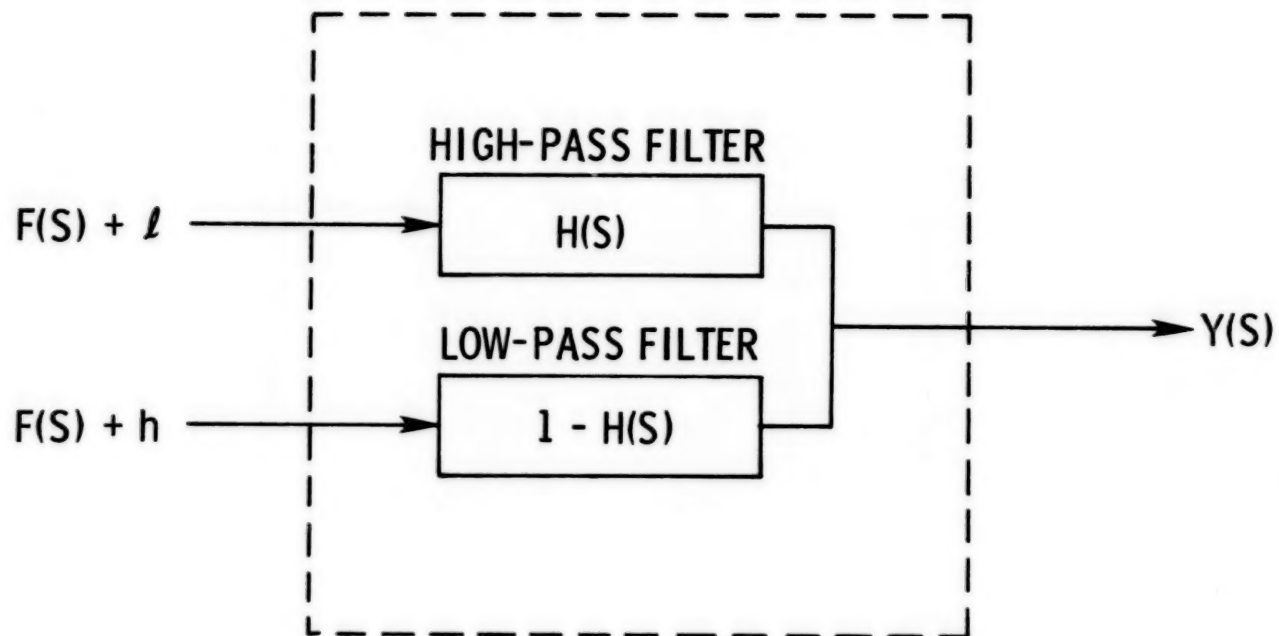
Figure 2.- Complementary filter with noisy inputs.

HIGH-PASS FILTER

$$\frac{TS}{TS + 1}$$

LOW-PASS FILTER

$$\frac{1}{TS + 1}$$

$F(S) + \ell$

$F(S) + h$

$Y(S)$
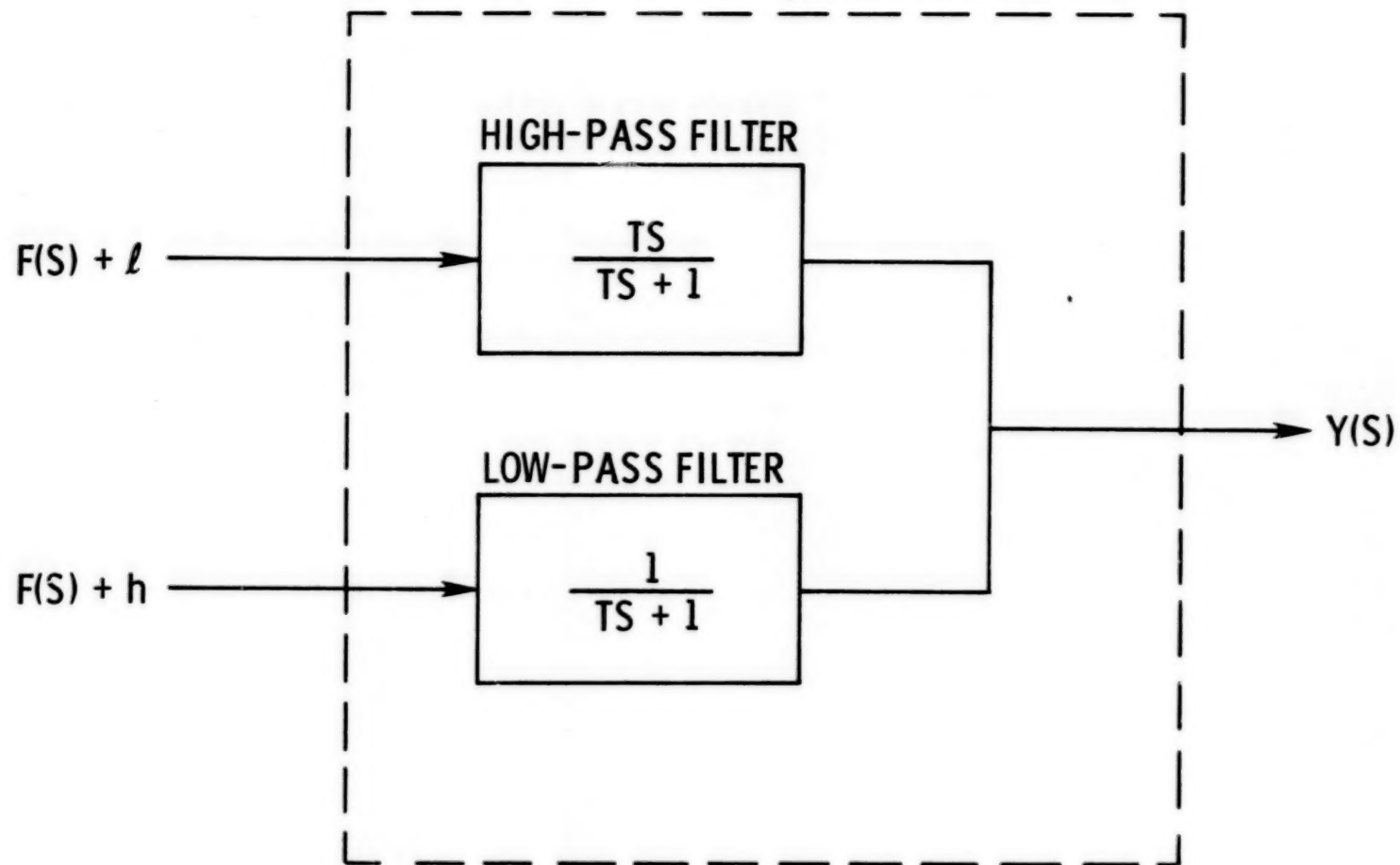
Figure 3.- Specific form of complementary filter.
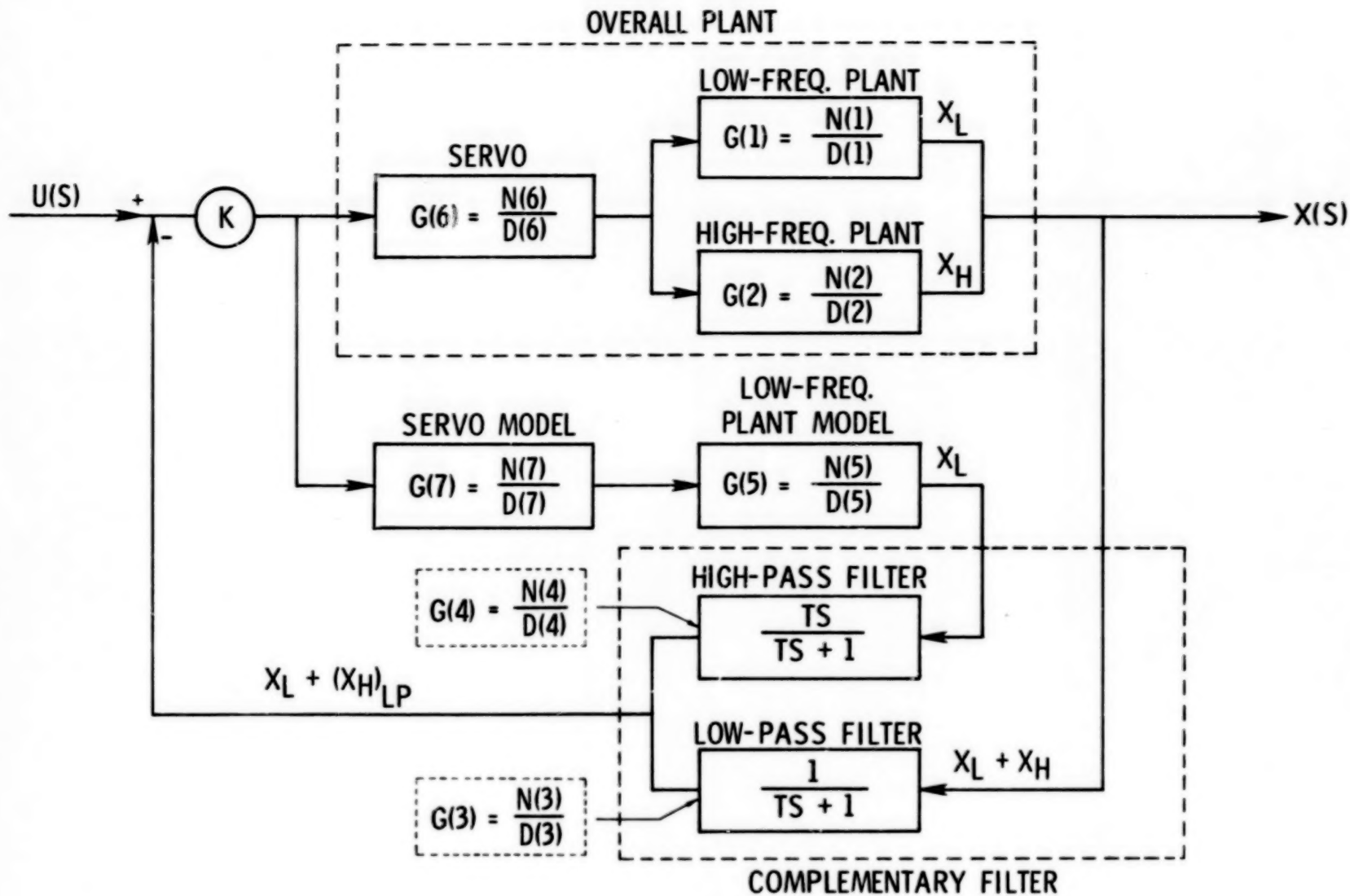
Figure 4.- System block diagram.
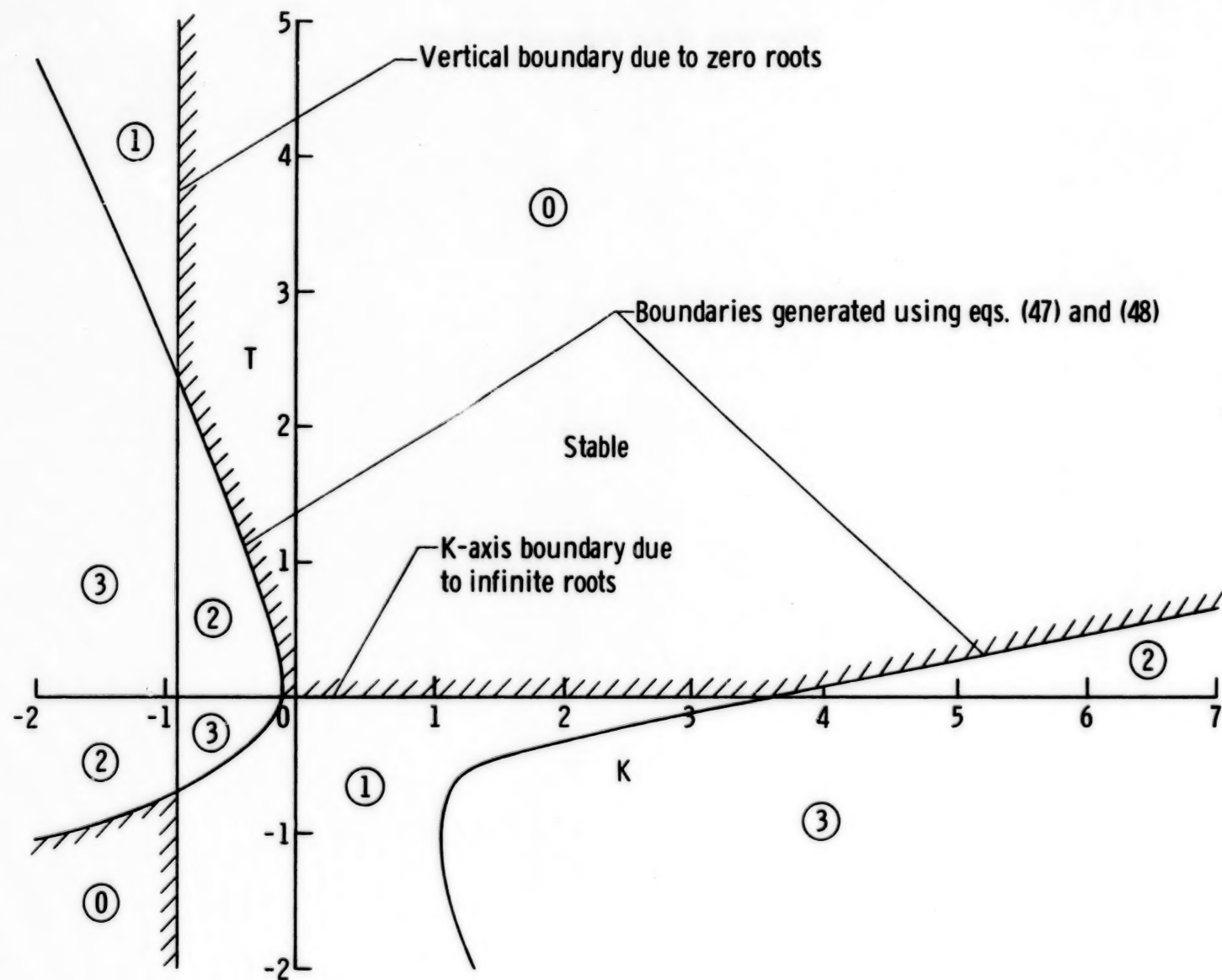
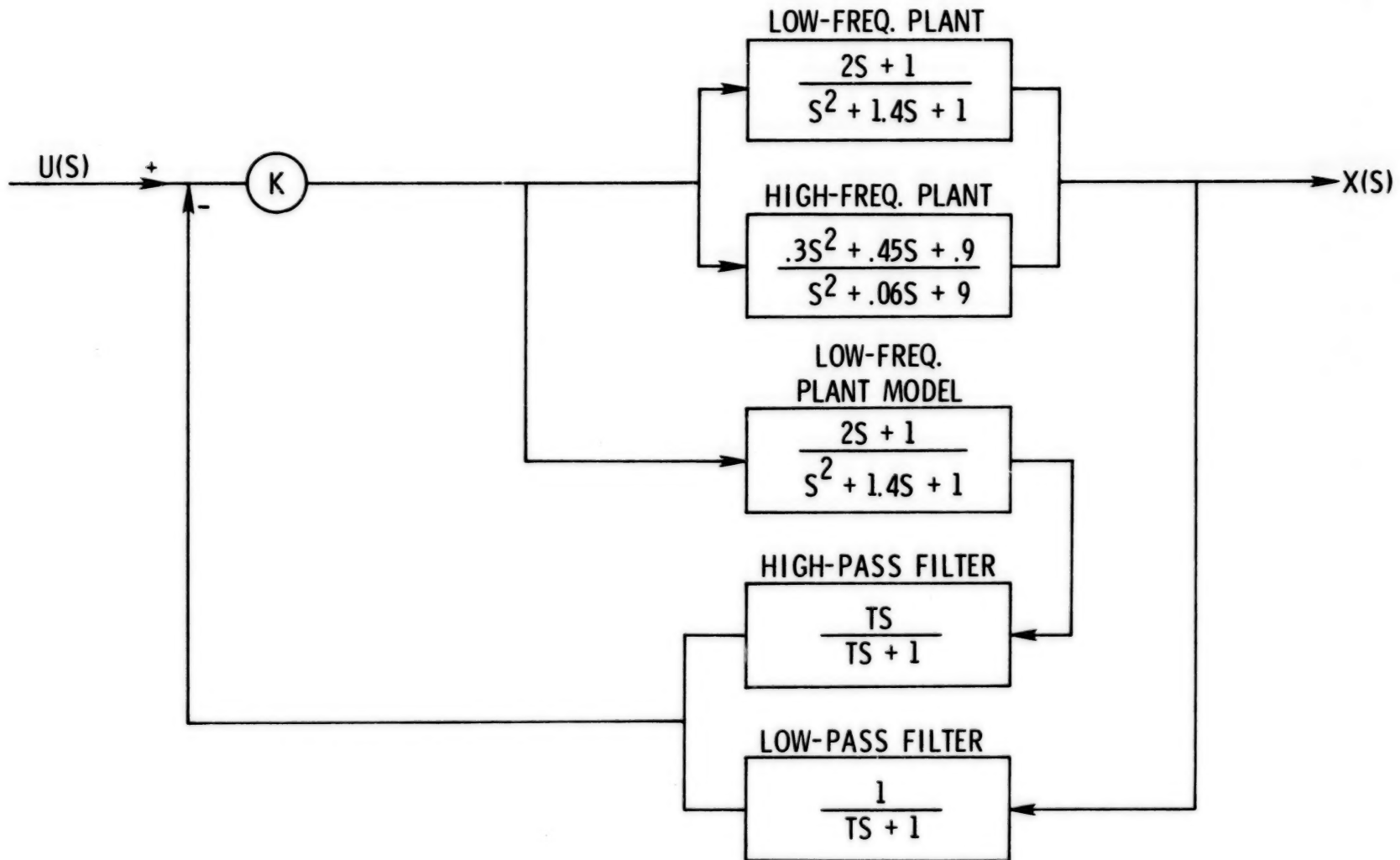Figure 5.- Sample stability boundaries with number of unstable roots circled in each region.
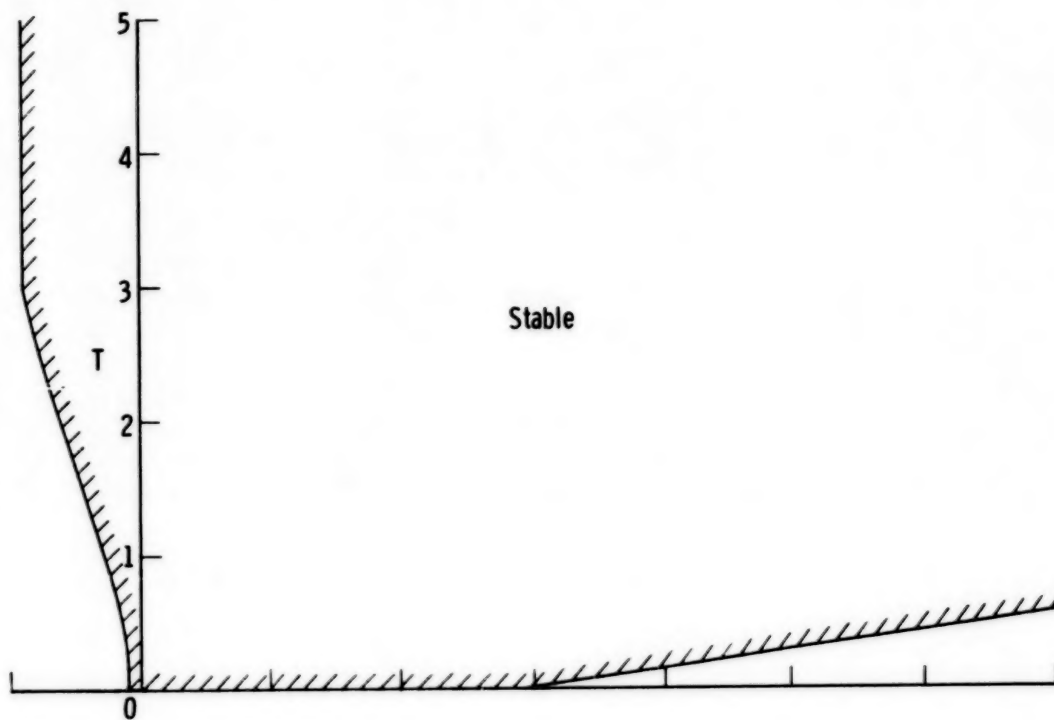
23

```
┌─────────────────────────────────────────────────────┐
│      Specify system transfer functions  (figure 4)   │
└─────────────────────────────────────────────────────┘
                           │
                           ▼
┌─────────────────────────────────────────────────────┐
│   Obtain values for:  $\omega$, M, $T_1$, $K_1$, $T_2$, $K_2$   │
│                 (Eqs.  (36), (37), (38))             │
└─────────────────────────────────────────────────────┘
                           │
                           ▼
┌─────────────────────────────────────────────────────┐
│      Plot stability boundaries (T versus K)          │
│                 (Eqs.  (36), (38))                   │
└─────────────────────────────────────────────────────┘
                           │
                           ▼
┌─────────────────────────────────────────────────────┐
│ Identify stable regions by computing characteristic roots │
│                       (Eq.  (20))                    │
└─────────────────────────────────────────────────────┘
```
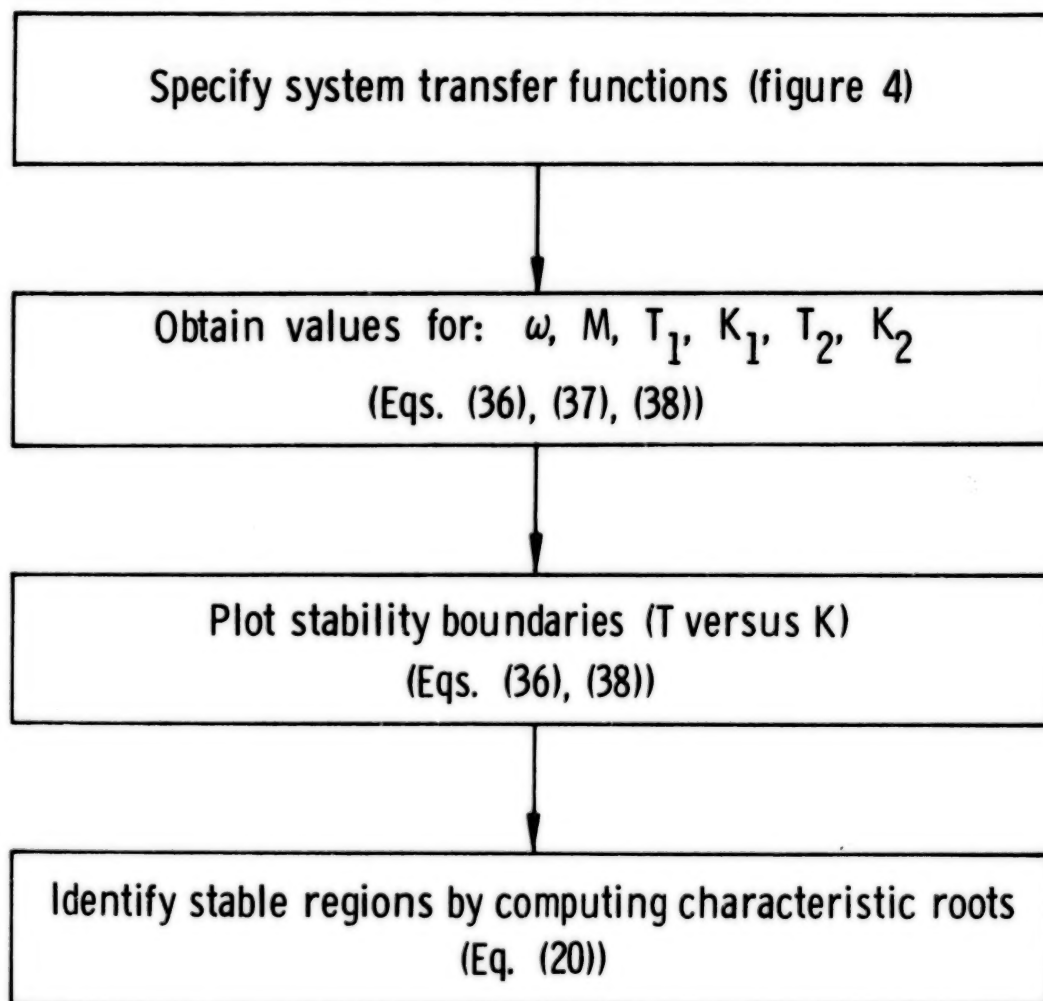
Figure 6.- Calculation procedure.

(a) Block diagram.

Figure 7.- Block diagram and stable regions for case 1 without servo.

(b) Stable region with low-pass filter.
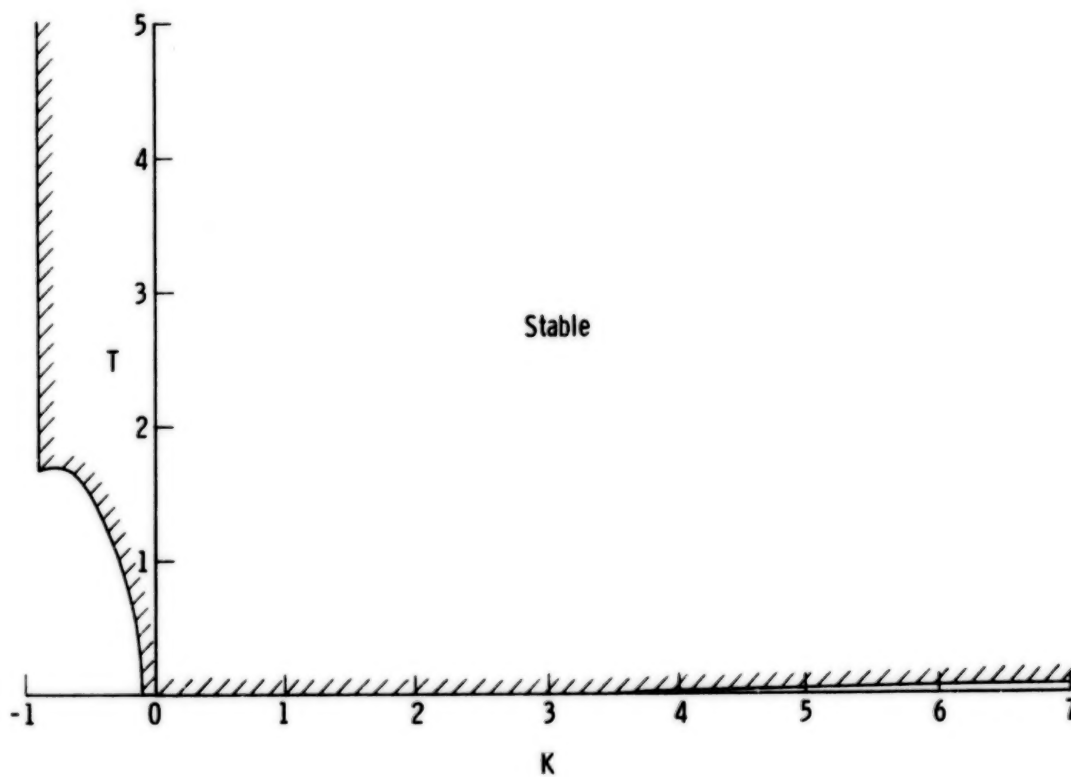
(c) Stable region with complementary filter.
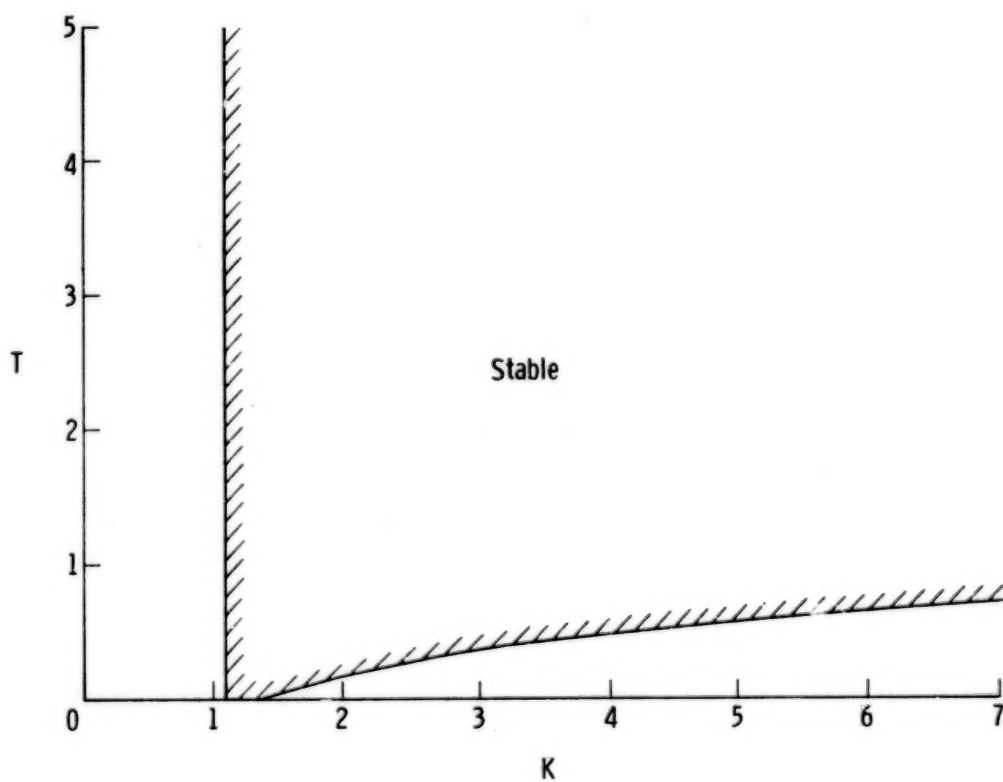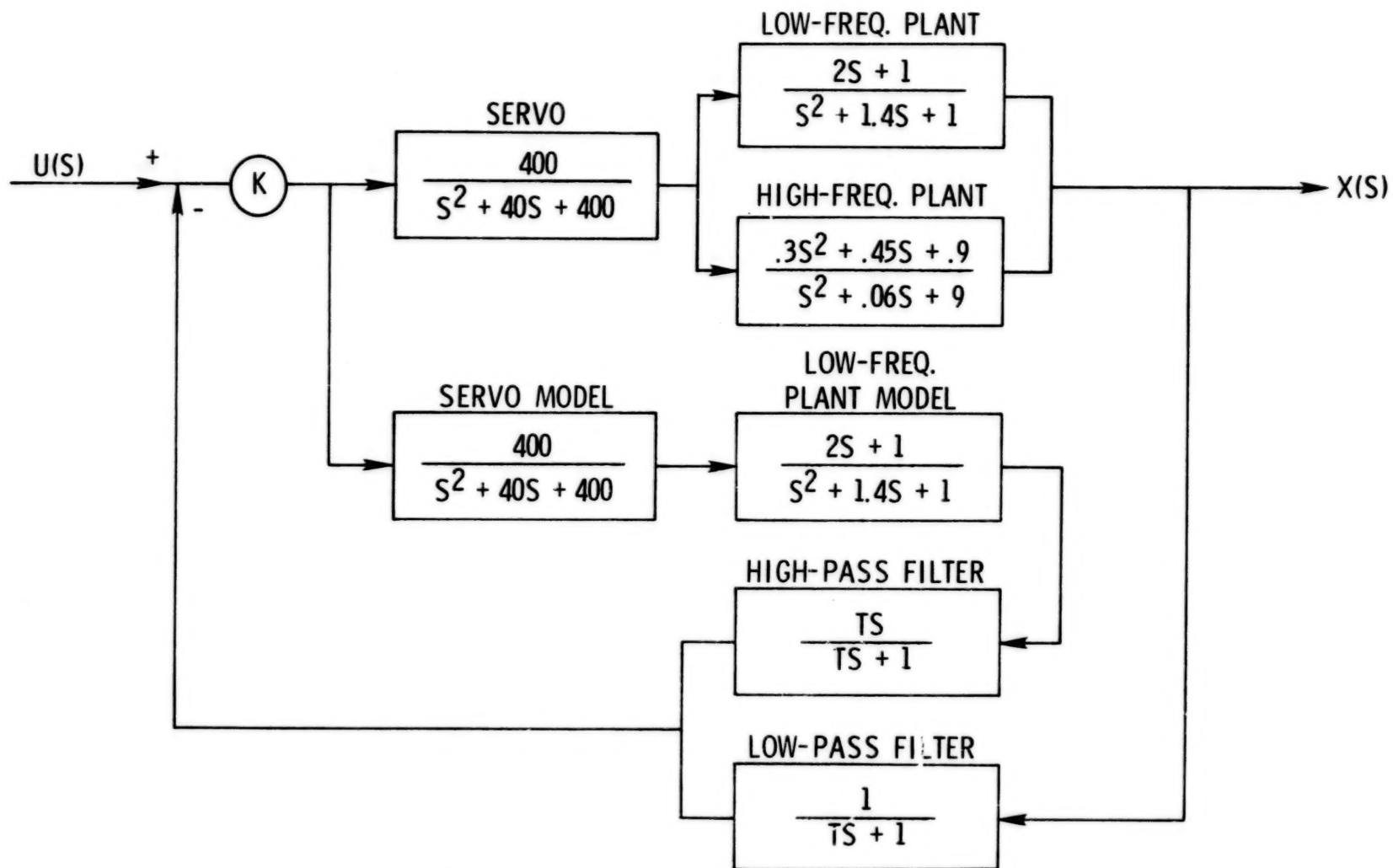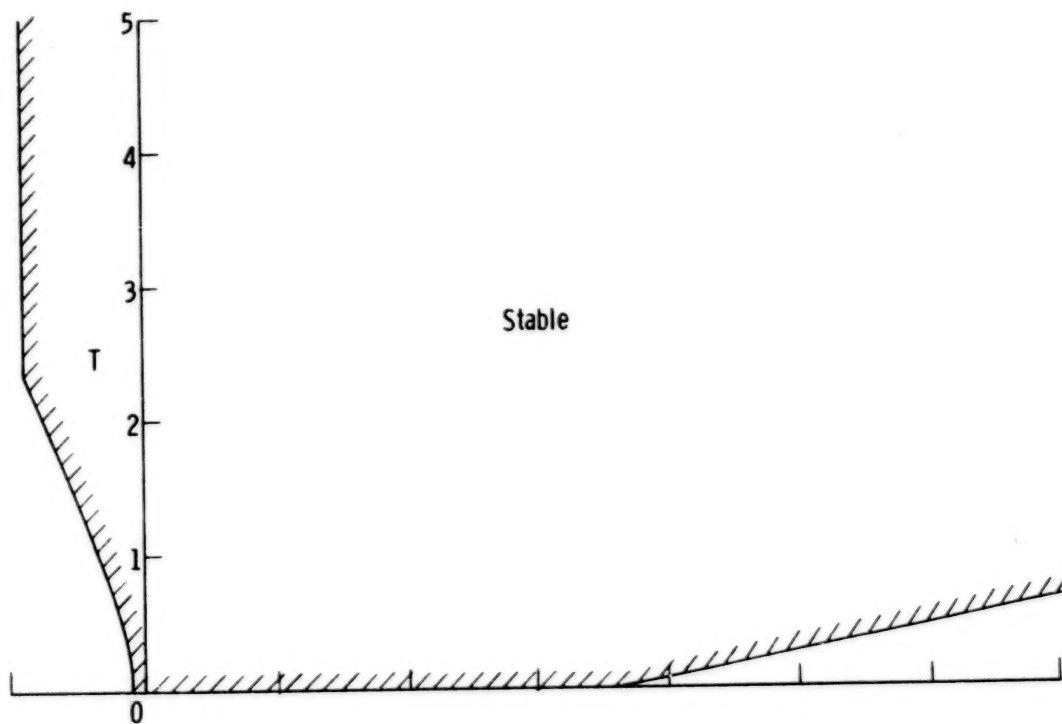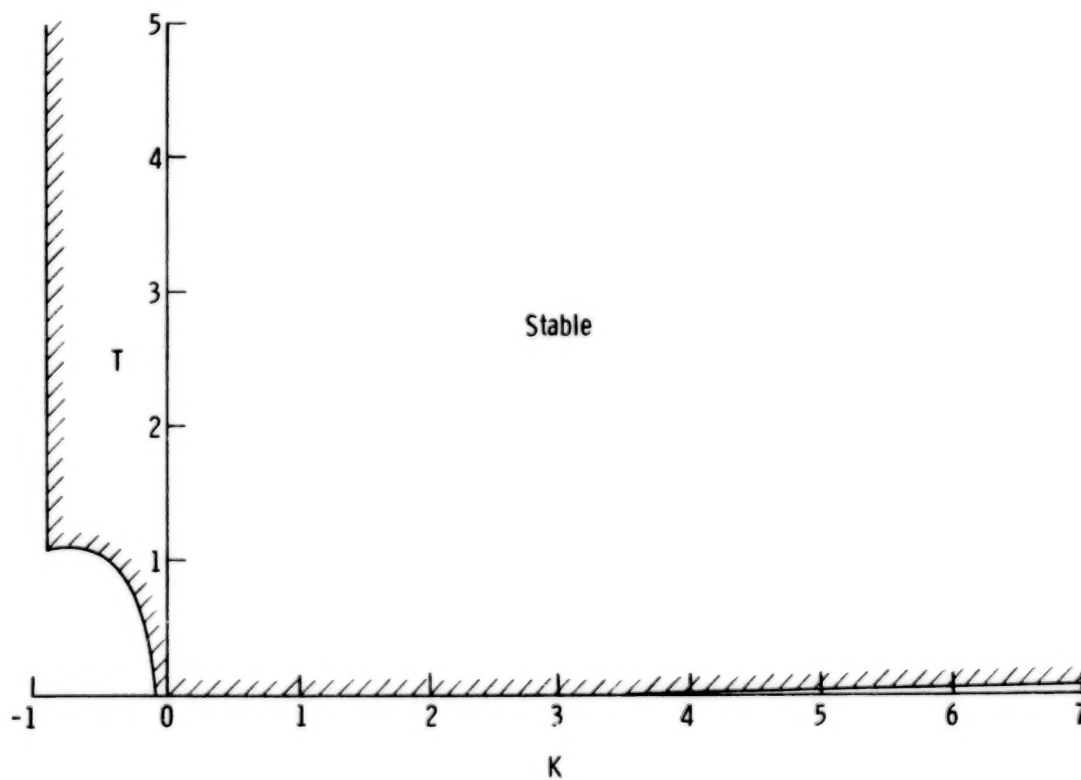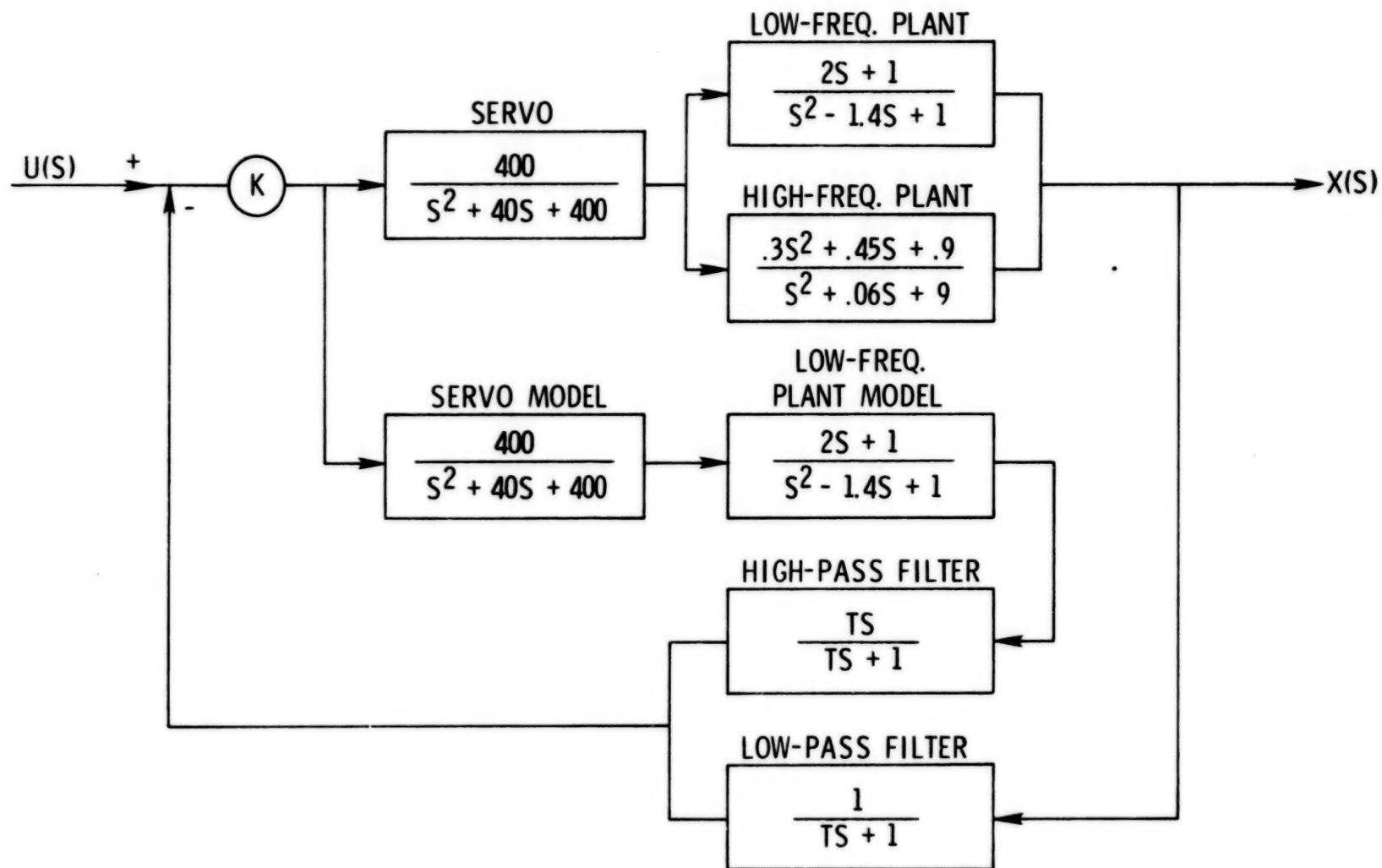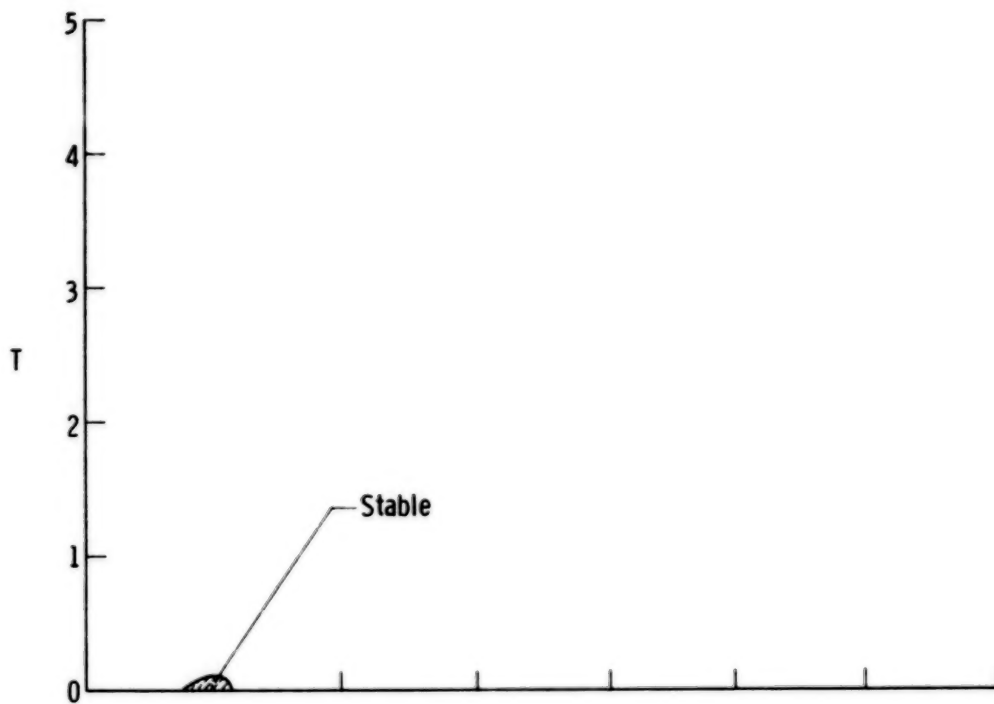
Figure 7.- Concluded.
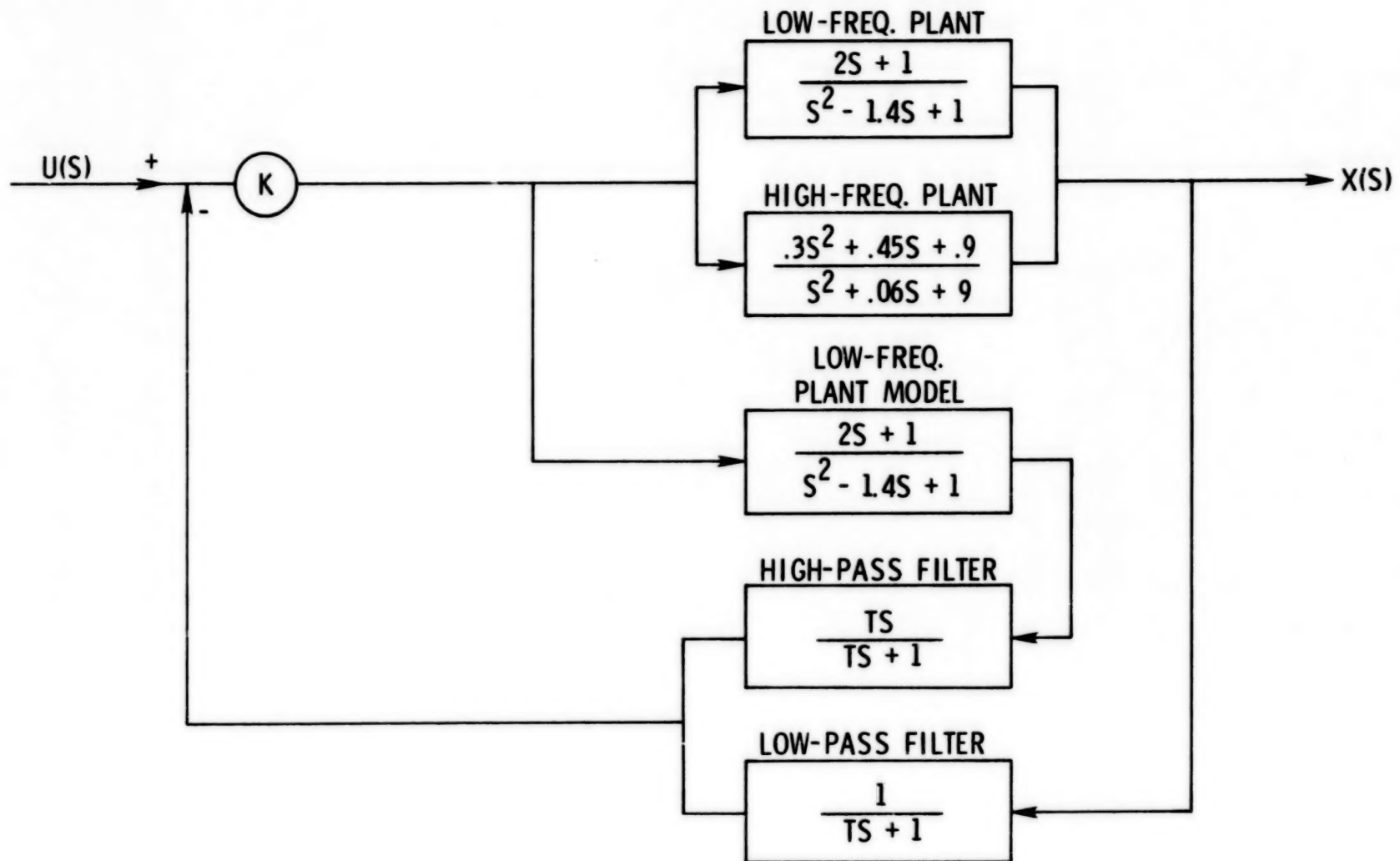
(a) Block diagram.

Figure 8.- Block diagram and stable regions for case 2 without servo.

27
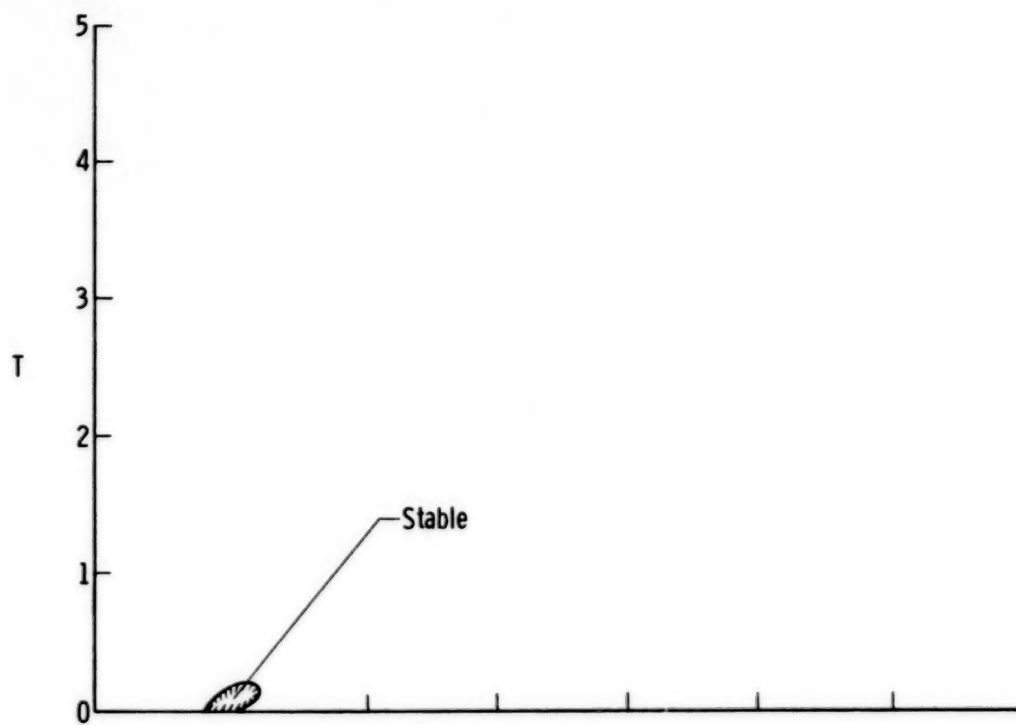
(b) Stable region with low-pass filter.
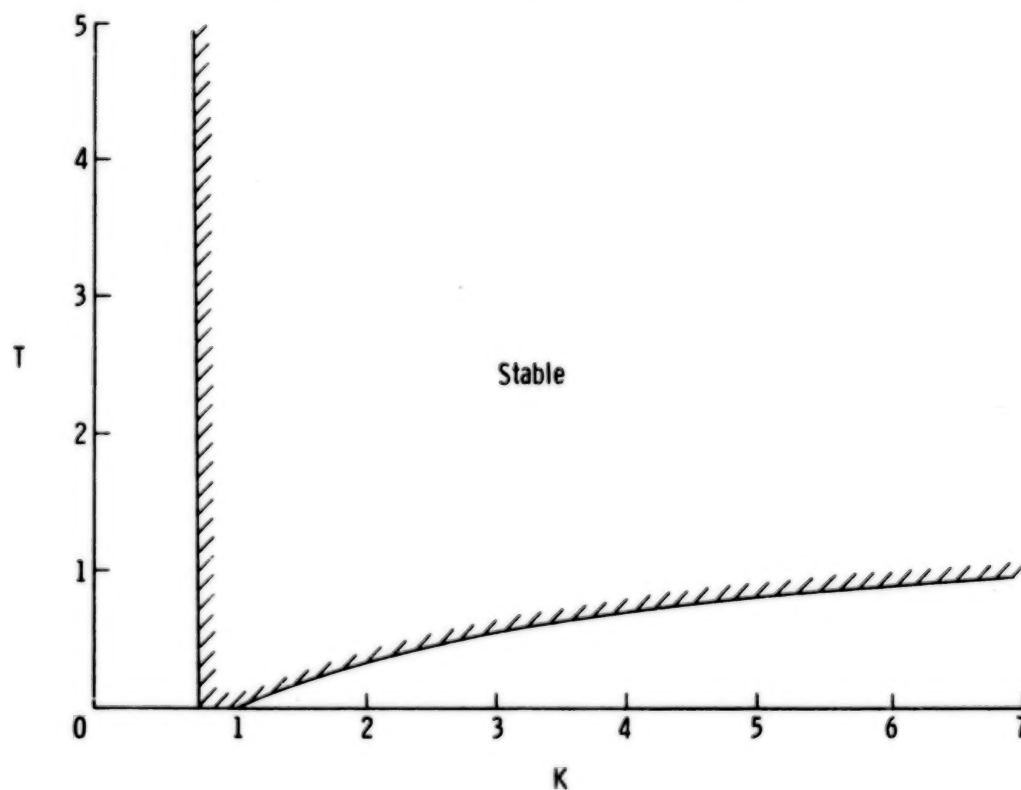
(c) Stable region with complementary filter.

Figure 8.- Concluded.
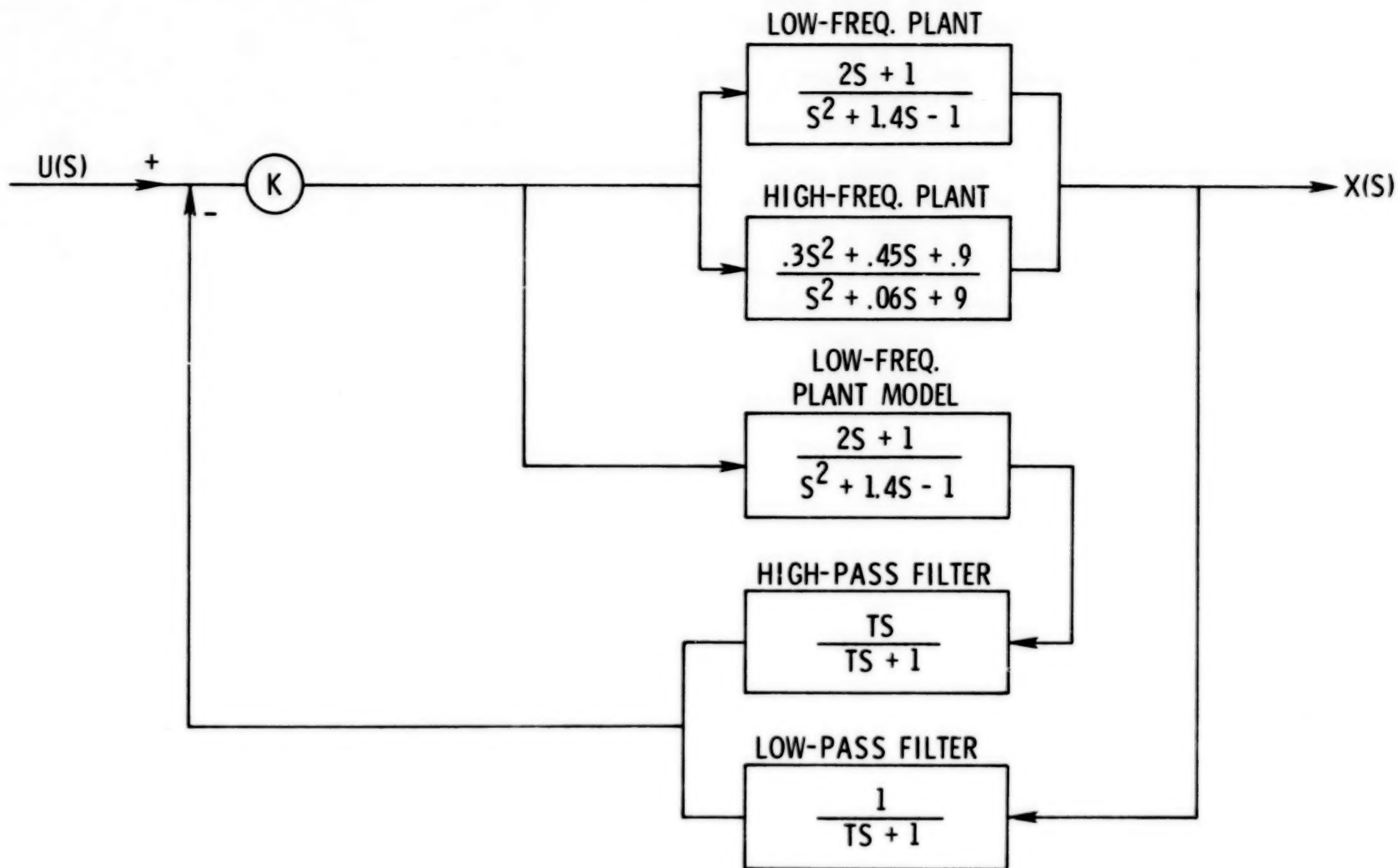
(a) Block diagram.

Figure 9.- Block diagram and stable regions for case 3 without servo.
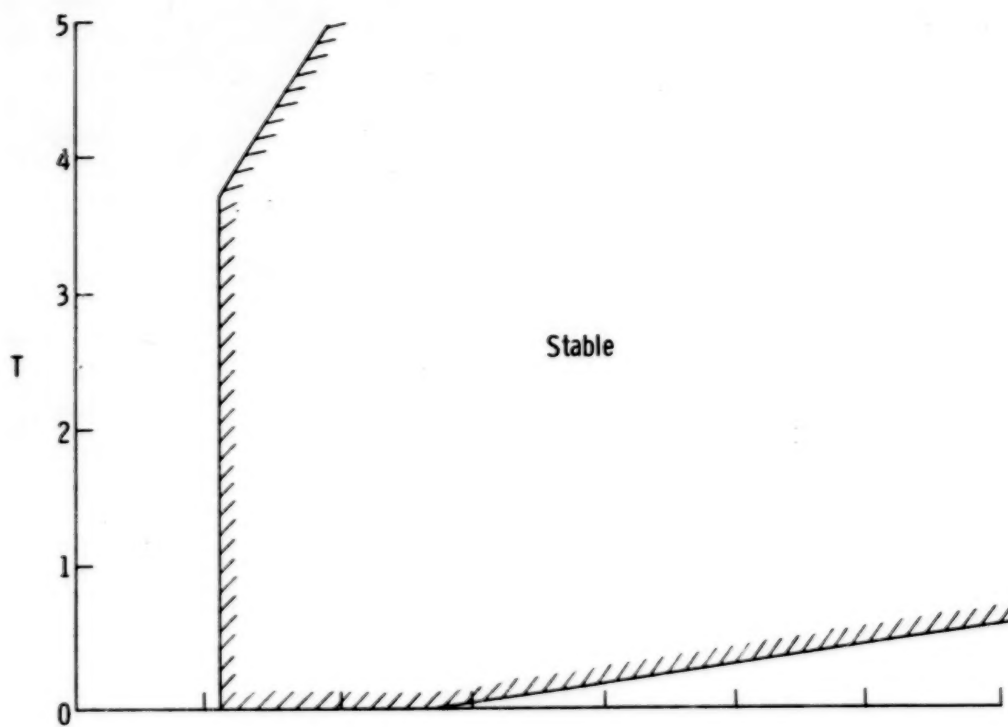
(b) Stable region with low-pass filter.
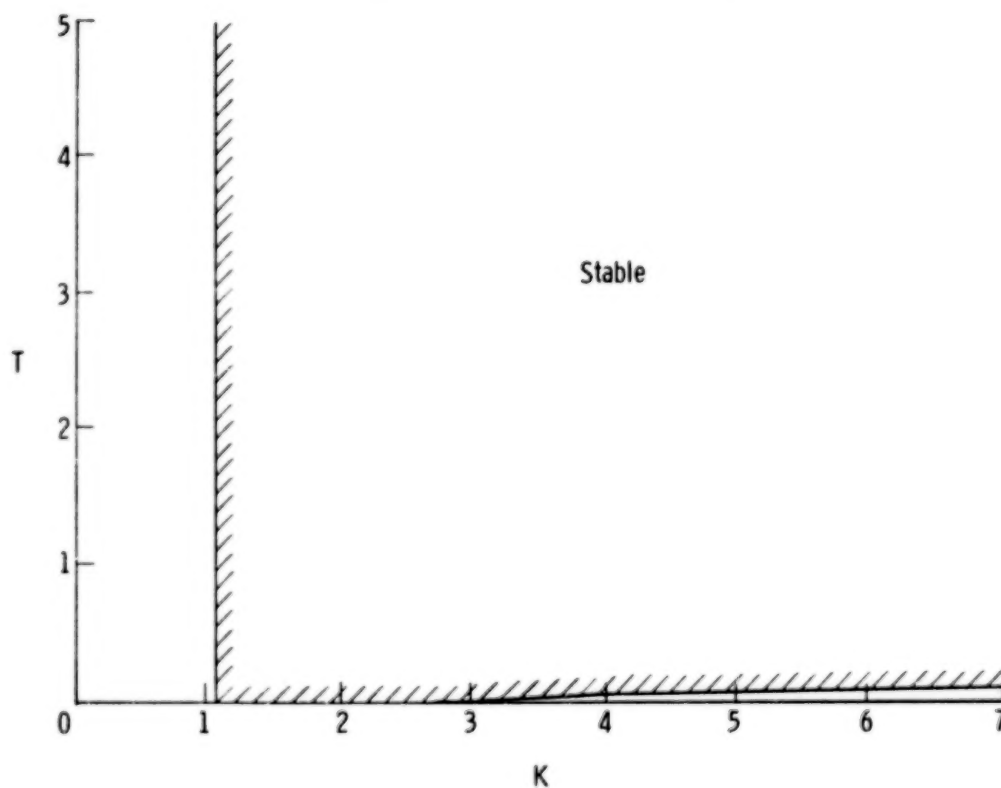
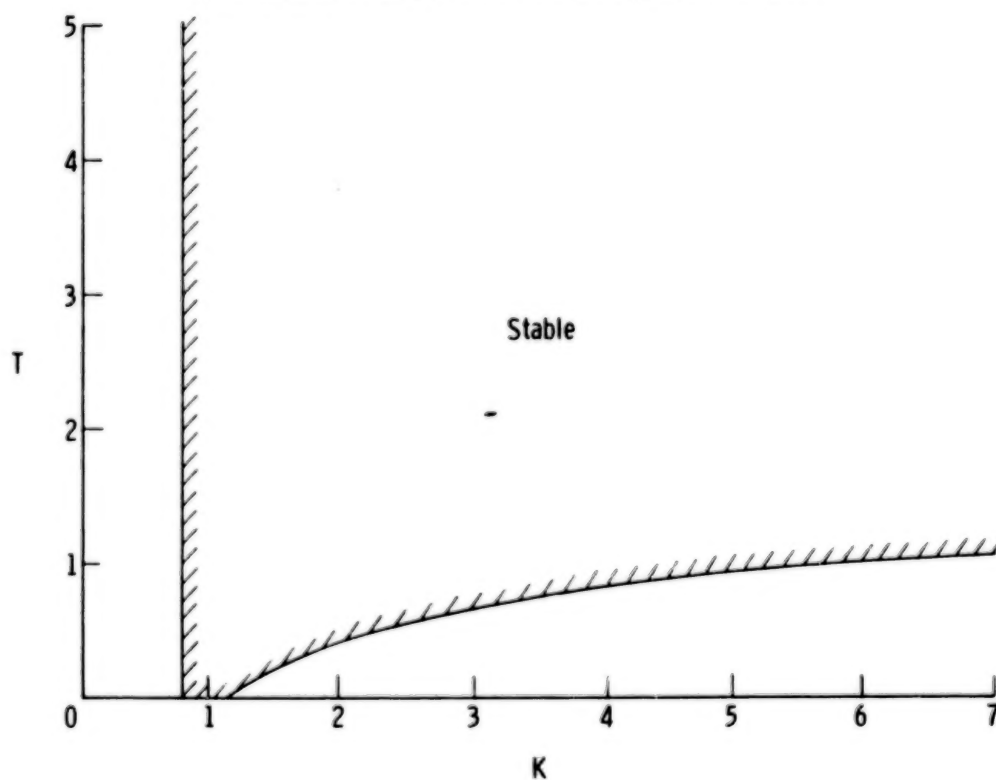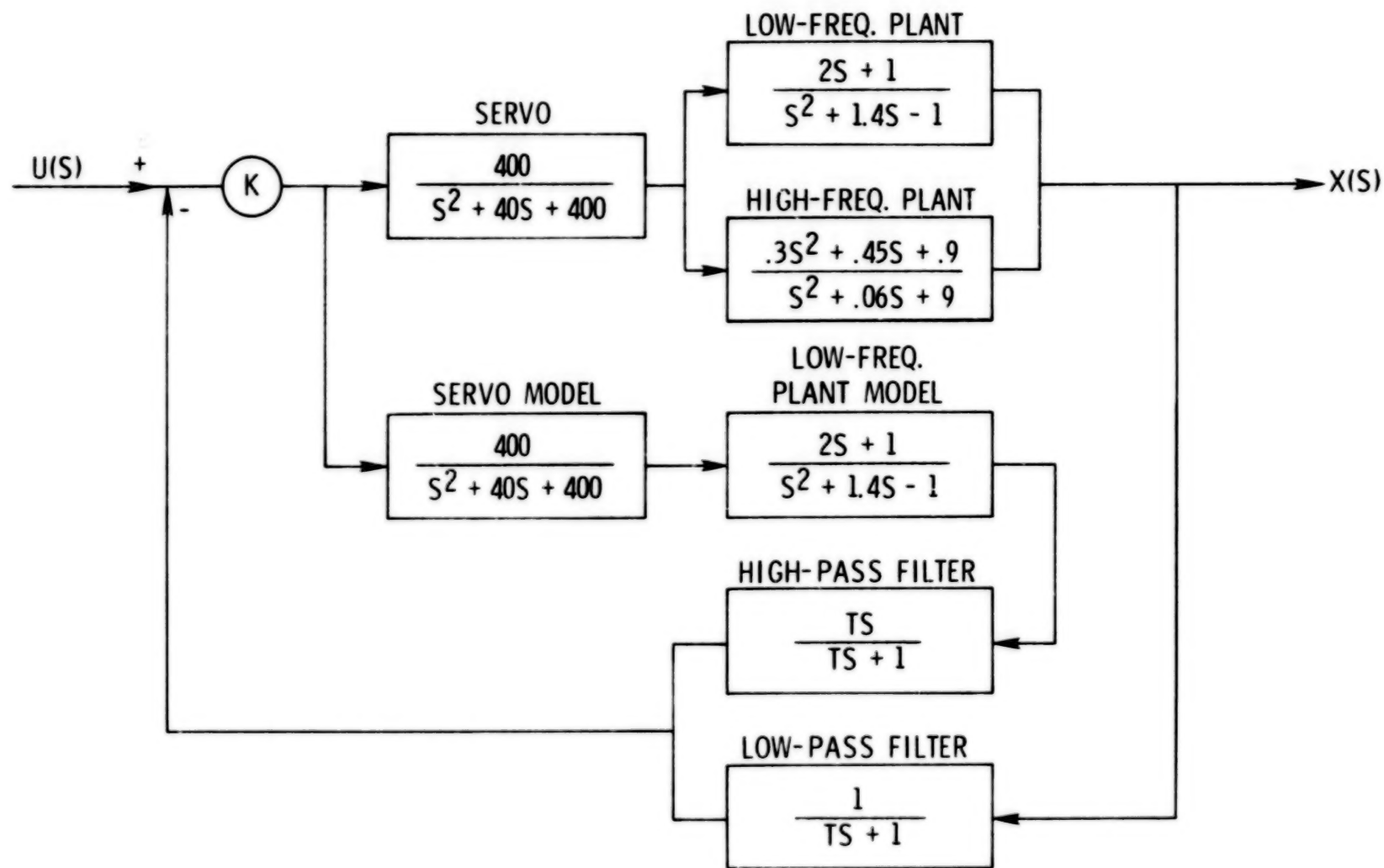(c) Stable region with complementary filter.

Figure 9.- Concluded.
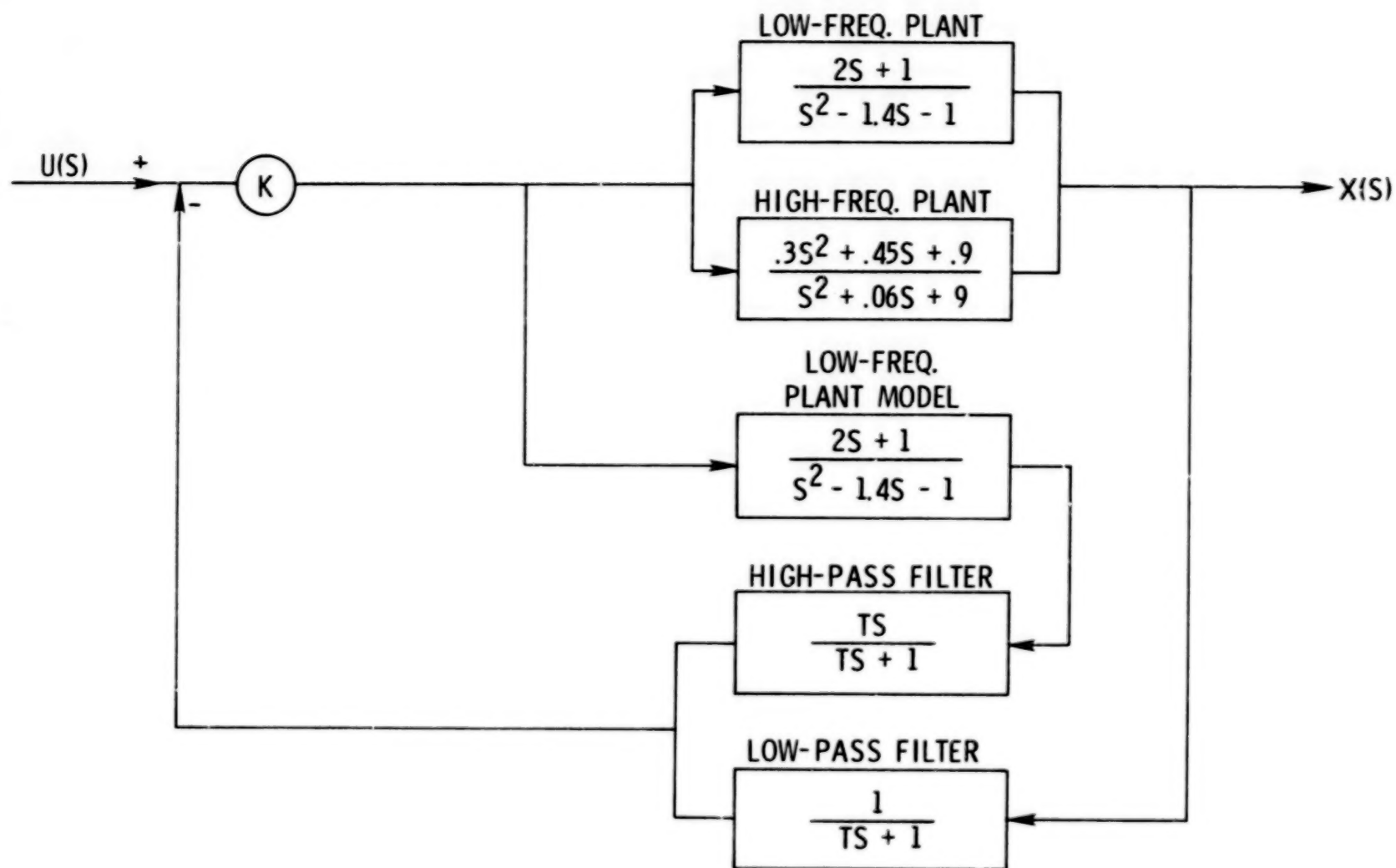
(a) Block diagram.

Figure 10.- Block diagram and stable regions for case 4 without servo.
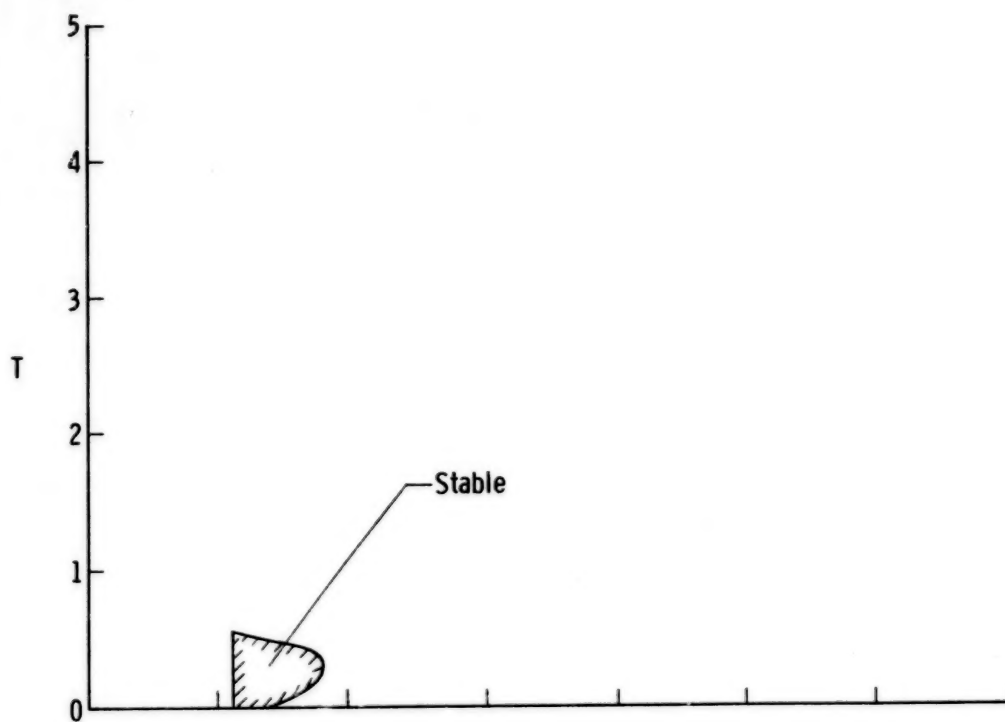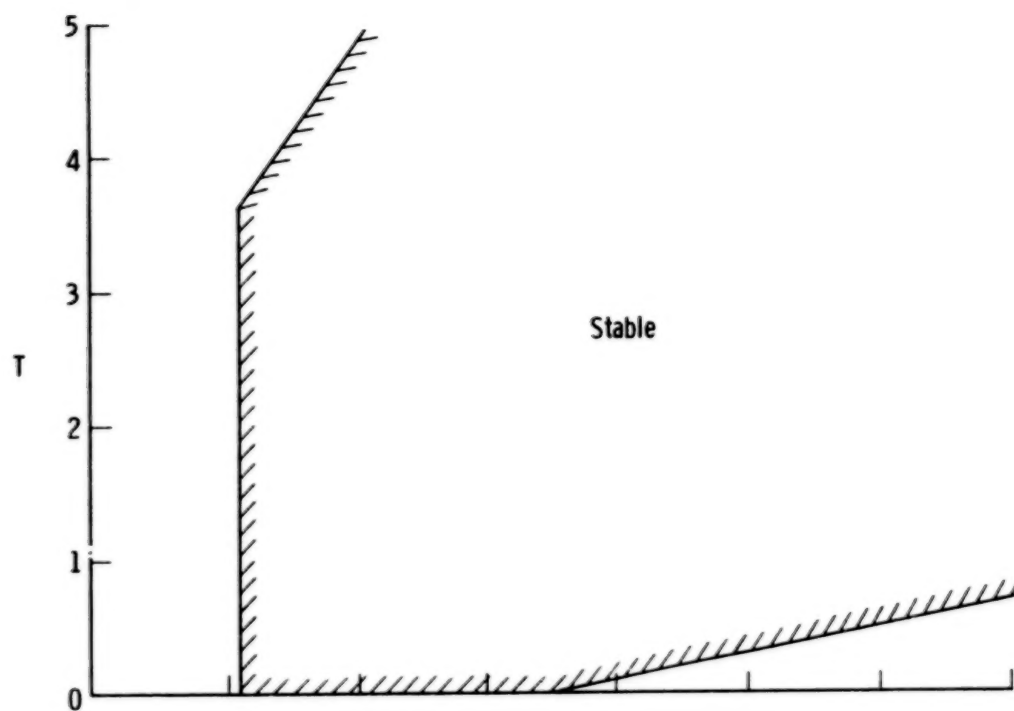
(b) Stable region with low-pass filter.

(c) Stable region with complementary filter.

Figure 10.- Concluded.

(a) Block diagram.

Figure 11.- Block diagram and stable regions for case 1 with servo.

(b) Stable region with low-pass filter.

(c) Stable region with complementary filter.

Figure 11.- Concluded.

(a) Block diagram.

Figure 12.– Block diagram and stable regions for case 2 with servo.

(b) Stable region with low-pass filter.

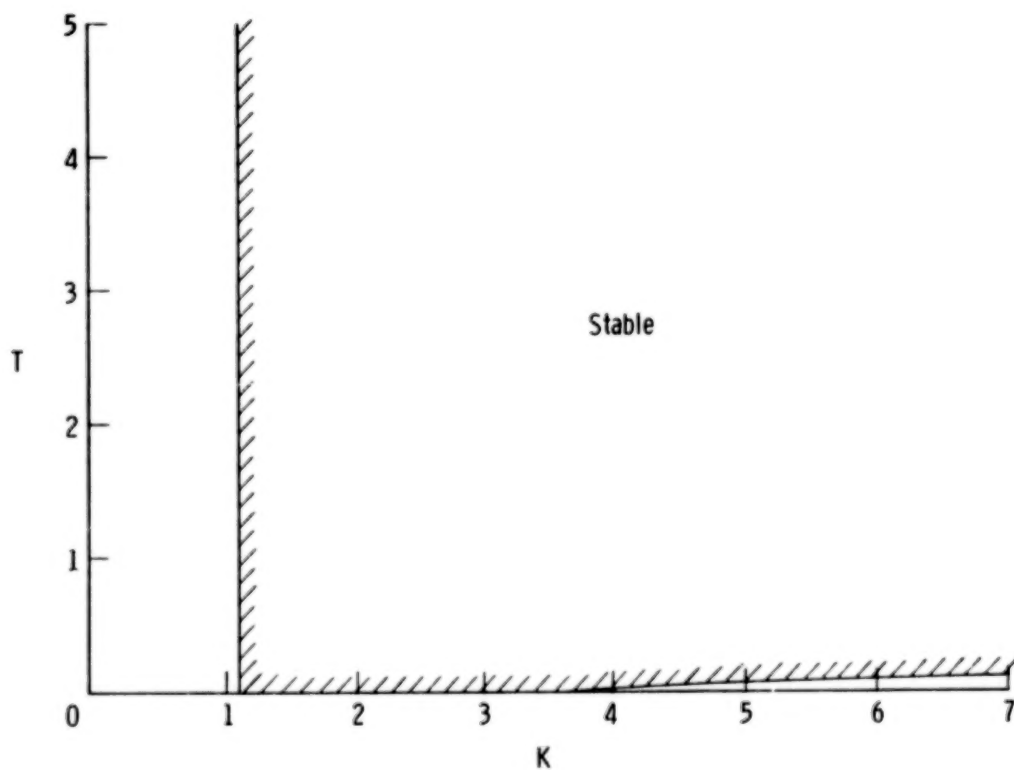(c) Stable region with complementary filter.

Figure 12.- Concluded.

(a) Block diagram.

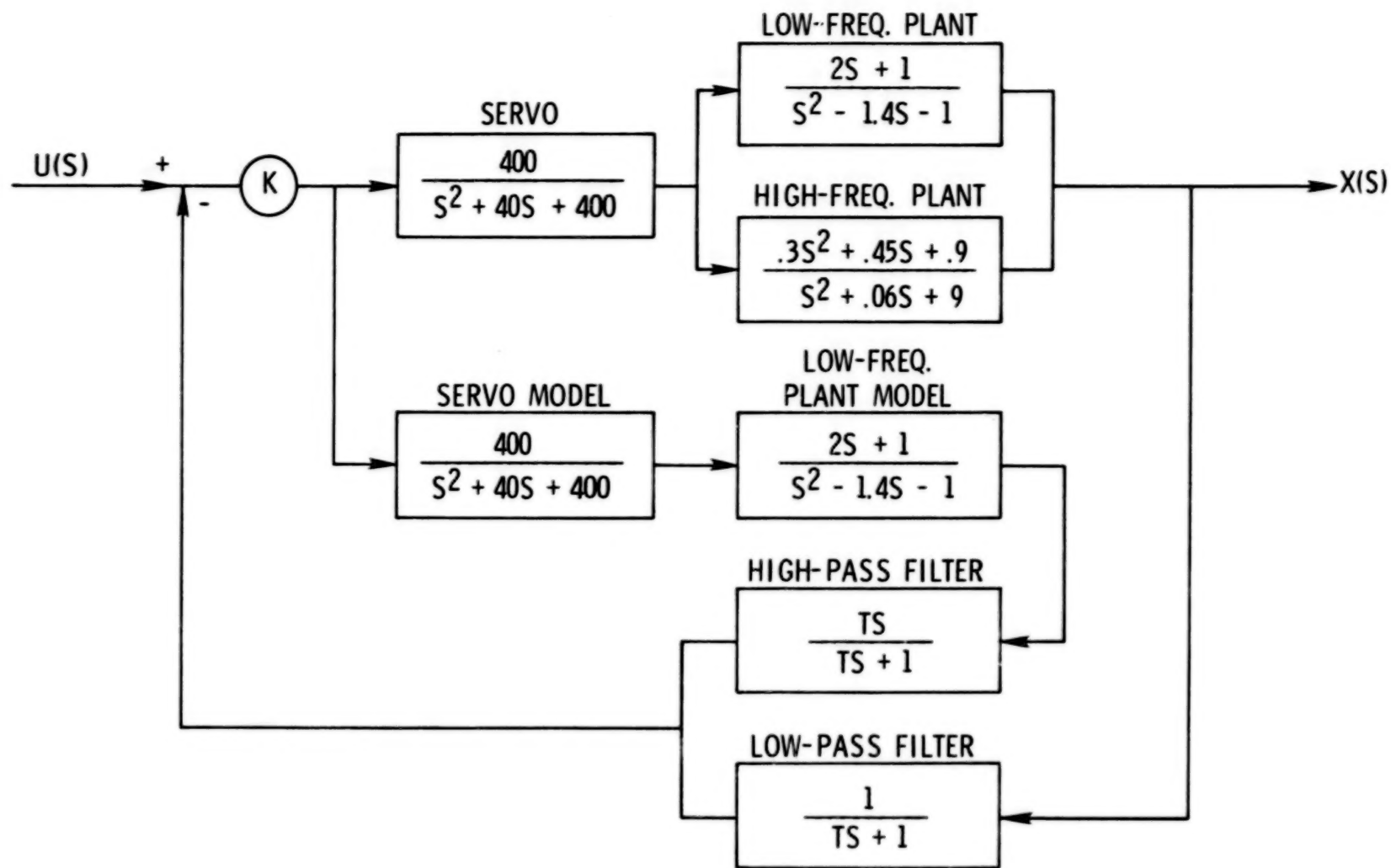Figure 13.- Block diagram and stable regions for case 3 with servo.
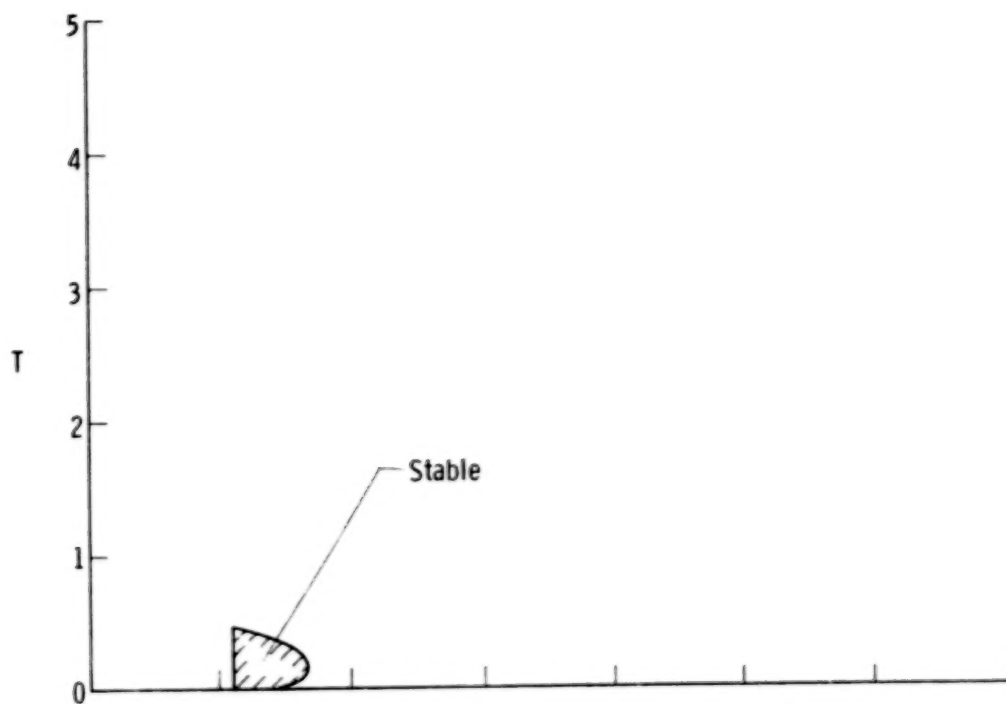
37

(b) Stable region with low-pass filter.

(c) Stable region with complementary filter.
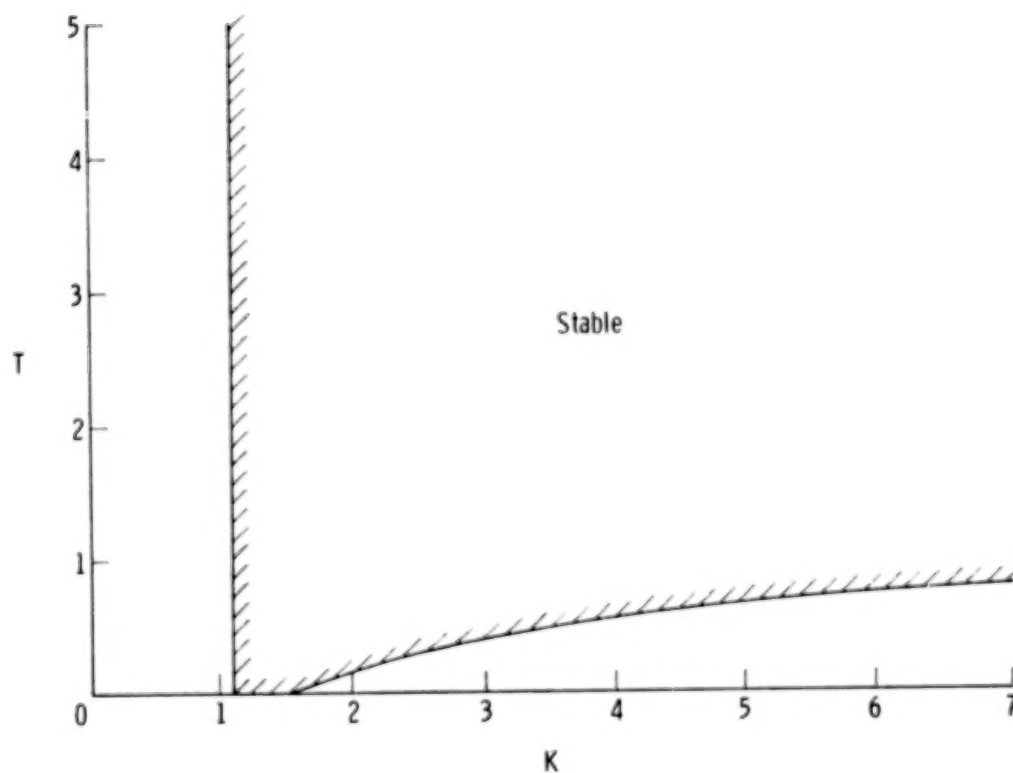
Figure 13.- Concluded.

(a) Block diagram.

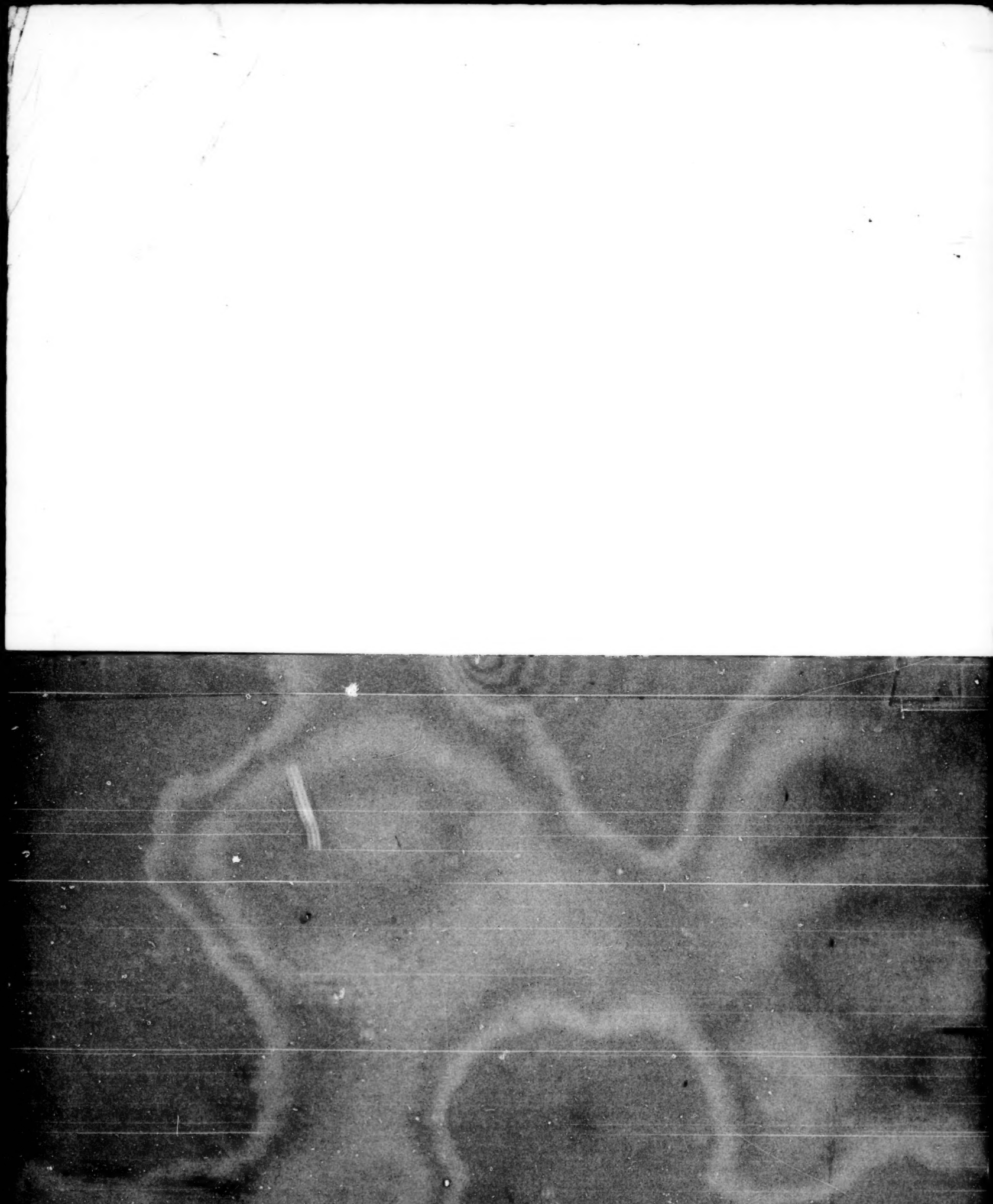Figure 14.- Block diagram and stable regions for case 4 with servo.

39

(b) Stable region with low-pass filter.

(c) Stable region with complementary filter.

Figure 14.- Concluded.

1. Report No. NASA TP-1744	2. Government Accession No.	3. Recipient's Catalog No.
4. Title and Subtitle STABILITY BOUNDARIES FOR SYSTEMS WITH FREQUENCY-MODEL FEEDBACK AND COMPLEMENTARY FILTER		5. Report Date **November 1980**
		6. Performing Organization Code
7. Author(s) L. Keith Barker		8. Performing Organization Report No. **L-13787**
9. Performing Organization Name and Address NASA Langley Research Center Hampton, VA 23665		10. Work Unit No. **506-54-13-02**
		11. Contract or Grant No.
12. Sponsoring Agency Name and Address National Aeronautics and Space Administration Washington, DC 20546		13. Type of Report and Period Covered **Technical Paper**
		14. Sponsoring Agency Code

15. Supplementary Notes

16. Abstract

General parameter-plane equations are derived to generate stability boundaries for a class of systems characterized by a feedback loop that contains a complementary filter and a model for either the low- or high-frequency portion of the plant. This combination allows those frequencies of the part of the plant that is modeled to be fed back for control while suppressing other frequencies. For all specific examples considered, the stability regions obtained using the complementary filter and frequency model were larger (and in some cases, considerably larger) than those obtained using a low-pass filter in the feedback of the system output. Furthermore, higher gain control was possible.

17. Key Words (Suggested by Author(s)) Complementary filter Parameter plane Stability boundaries Frequency model feedback High-gain control	18. Distribution Statement Unclassified - Unlimited Subject Category 66

19. Security Classif. (of this report) Unclassified	20. Security Classif. (of this page) Unclassified	21. No. of Pages 40	22. Price A03

END

March 6, 1981